comptes rendus palevol

2026 • 25 • 18

A new fossil buffalo from the Shungura Formation (Ethiopia) reveals the role of heterochrony in the evolution of *Syncerus* Hodgson, 1847

Faysal BIBI & Jean-Renaud BOISSERIE

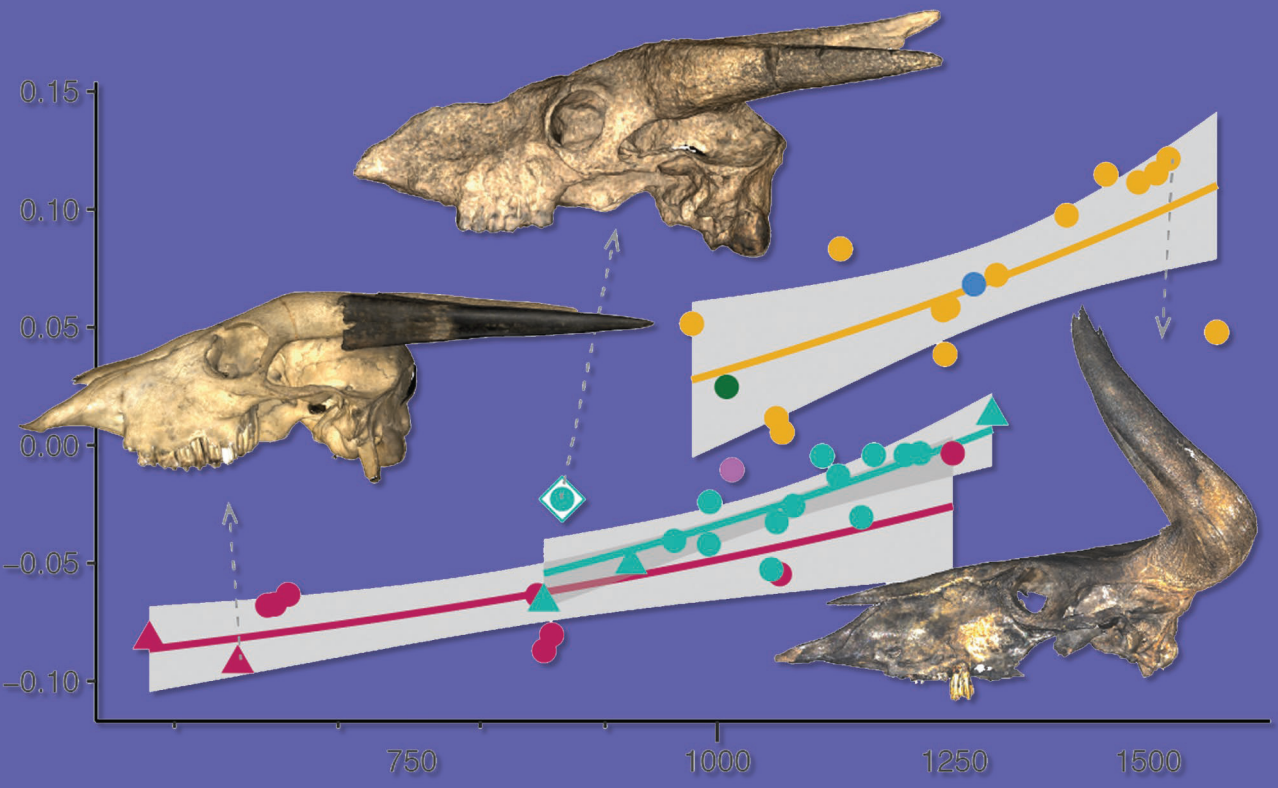

GLIMPSES OF A PLIO-PLEISTOCENE AFRICAN ECOSYSTEM: THE LOWER OMO VALLEY, ETHIOPIA

Edited by Jean-Renaud BOISSERIE, Aurélien MOUNIER, Blade Engda REDAE & Mathieu SCHUSTER

art. 25 (18) — Published on 29 September 2026
www.cr-palevol.fr

PUBLICATIONS SCIENTIFIQUES

ISSN (imprimé / *print*) : 1631-0683/ ISSN (électronique / *electronic*) : 1777-571X

A new fossil buffalo from the Shungura Formation (Ethiopia) reveals the role of heterochrony in the evolution of *Syncerus* Hodgson, 1847

Faysal BIBI
Museum für Naturkunde, Leibniz Institute for Evolution and Biodiversity Science,
Invalidenstrasse 43, 10115 Berlin (Germany)
faysal.bibi@mfn.berlin (corresponding author)

Jean-Renaud BOISSERIE
Centre Français des Études Éthiopiennes, CNRS,
Ministère de l'Europe et des affaires étrangères, PO BOX 5554 Addis Ababa (Ethiopia)
and Laboratoire Paléontologie Évolution Paléoécosystèmes Paléoprimatologie, Laboratoire Paléontologie Evolution Paléoécosystèmes Paléoprimatologie (PALEVOPRIM), CNRS,
Université de Poitiers, 6 rue Michel Brunet, 86073 Poitiers (France)
jean.renaud.boisserie@univ-poitiers.fr

Submitted on 19 November 2025 | Accepted on 9 March 2026 | Published on 29 September 2026

urn:lsid:zoobank.org:pub:88113219-D1DA-4ACC-B519-7B6AEA353ED2

Bibi B. & Boisserie J.-R. 2026. — A new fossil buffalo from the Shungura Formation (Ethiopia) reveals the role of heterochrony in the evolution of *Syncerus* Hodgson, 1847, *in* Boisserie J.-R., Mounier A., Redae B. E. & Schuster M. (eds), Glimpses of a Plio-Pleistocene African ecosystem: the Lower Omo Valley, Ethiopia. *Comptes Rendus Palevol* 25 (18): 319-356. https://doi.org/10.5852/cr-palevol2026v25a18

ABSTRACT
Variation in the timing and rate of development (heterochrony) is a key driver of morphological diversification. The African buffalo (*Syncerus caffer* (Sparrman, 1779)) is the sole surviving species of a once diverse Pleistocene clade and shows striking eco-morphological variability that may be the result of heterochronic shifts. Heterochrony has also been suspected to account for the past diversity of *Syncerus*, but the early evolution of this clade has remained obscure due to limited fossil evidence. Here we describe new material from the Shungura Formation (southern Ethiopia), including a nearly complete cranium dated to *c.* 2.6 Ma, which we designate as the type of a new species of *Syncerus* Hodgson, 1847. This species is small-bodied with short, divergent horns, resembling immature and small-bodied extant *Sy. caffer* (forest or "nanus" ecomorphs). Three-dimensional geometric morphometrics reveal that fossils of *Ugandax* Cooke & Coryndon, 1970 and *Syncerus* (including the new cranium) broadly follow the ontogenetic size-shape allometry of *Sy. caffer*, suggesting cranial diversification along a conserved allometric trajectory, and that the new species may represent an ancestral form from which later *Syncerus* evolved. In contrast, the extreme horn length of the extinct giant buffalo *Sy. antiquus* (Duvernoy, 1851) departs from this pattern, indicating lineage-specific innovation. These findings provide the earliest well-preserved evidence of the African buffalo lineage and highlight the role of conserved allometry and heterochrony in the evolutionary history of *Syncerus*. They also underscore the importance of new fossil discoveries and comparative analyses for understanding the origins of morphological diversity.

KEY WORDS
Syncerus,
Bovidae,
Pliocene,
Pleistocene,
Africa,
geometric
morphometrics,
heterochrony,
new species.

RÉSUMÉ
Un nouveau buffle fossile de la Formation de Shungura (Éthiopie) révèle le rôle de l'hétérochronie dans l'évolution de Syncerus *Hodgson, 1847.*
Les variations du rythme et de la durée du développement (hétérochronies) constituent un moteur essentiel de la diversification morphologique. Le buffle d'Afrique (*Syncerus caffer* (Sparrman, 1779)), seul survivant d'un clade pléistocène autrefois diversifié, présente une remarquable variabilité écomorphologique qui pourrait résulter de décalages hétérochroniques. Les hétérochronies ont également été proposées pour expliquer la diversité passée de *Syncerus*, mais l'évolution initiale de ce clade est restée méconnue en raison de la rareté des fossiles. Nous décrivons ici du matériel inédit provenant de la Formation de Shungura (sud-ouest de l'Éthiopie), dont un crâne sub-complet daté d'environ 2,6 Ma, que nous désignons comme type d'une nouvelle espèce de *Syncerus* Hodgson, 1847. Cette espèce est de petite taille et porte des cornes courtes et divergentes, rappelant les individus juvéniles et de petite taille de l'actuel *Sy. caffer* (écotype forestier ou « nanus »). Les analyses en morphométrie géométrique tridimensionnelle révèlent que les fossiles d'*Ugandax* Cooke & Coryndon, 1970 et de *Syncerus* (y compris le nouveau crâne) suivent de manière générale l'allométrie ontogénétique liant la taille et la forme chez *Sy. caffer*, ce qui suggère une diversification crânienne suivant une trajectoire allométrique identique, et que la nouvelle espèce pourrait représenter une forme ancestrale dont les représentants ultérieurs de *Syncerus* auraient dérivé. En revanche, la longueur extrême des cornes du buffle géant éteint *Sy. antiquus* (Duvernoy, 1851) s'écarte de ce schéma, indiquant une innovation spécifique à cette lignée. Ces résultats apportent le plus ancien témoignage bien préservé de la lignée du buffle d'Afrique et mettent en évidence le rôle de l'allométrie et des hétérochronies dans l'histoire évolutionnaire de *Syncerus*. Ils soulignent également l'importance de nouvelles découvertes fossiles et d'analyses comparatives pour comprendre les origines de la diversité morphologique.

MOTS CLÉS
Syncerus,
Bovidae,
Pliocène,
Pléistocène,
Afrique,
morphométrie
géométrique,
hétérochronie,
espèce nouvelle.

INTRODUCTION

Changes in organismal form are often tightly linked to changes in size, with allometric relationships explaining much of the morphological variation observed within and among species (Huxley 1932; Gould 1977; Klingenberg 2016; Cardini 2019). Such patterns frequently arise through heterochrony – shifts in the rate or timing of development – that move individuals or lineages along pre-existing size-shape trajectories and generate novel phenotypes (Simons & Frost 2021; Tejero-Cicuéndez *et al.* 2023). Although heterochrony is an important mechanism for morphological diversification, its role in shaping evolutionary lineages is often difficult to evaluate in the fossil record, especially where well-preserved specimens suitable for morphometric analysis are rare (Bhullar *et al.* 2012; Gomes Rodrigues *et al.* 2018; Krone *et al.* 2019; Kammerer *et al.* 2020).

The African buffalo, *Syncerus caffer* (Sparrman, 1779), provides a compelling case study. As the only living representative of an otherwise diverse Plio-Pleistocene radiation of African bovins, it exhibits striking phenotypic variability across its geographic range, from large, dark savanna buffalo with massive horns to small, reddish forest forms with short horns (Grubb 1972; Prins & Sinclair 2013). This remarkable variation has raised questions about the developmental and evolutionary processes underlying the lineage. Some evidence suggests that both extinct and extant *Syncerus* Hodgson, 1847 species may have diversified along conserved allometric trajectories, but the early history of the clade remains poorly documented due to the scarcity of well-preserved specimens.

Here we report a nearly complete cranium from the Shungura Formation (*c.* 2.6 Ma), which, together with associated horn cores, allows us to describe the earliest recognized species of *Syncerus*. This discovery not only clarifies the origins of the lineage but also provides a rare opportunity to evaluate the role of heterochrony and allometric scaling in the diversification of African buffalo. Using 3D geometric morphometrics, we assess cranial shape and size relationships across extant and extinct members of *Syncerus* and its relatives, testing whether their morphological disparity can be explained by shared ontogenetic and evolutionary allometries. Specifically, we tested the hypothesis that species of *Syncerus* are "scaled variants" of each other (Simons & Frost 2021). This predicts that fossil and recent *Syncerus* individuals share a common ontogenetic and evolutionary allometry and that the new fossil cranium aligns with the same size-shape relationship defined by extant *Sy. caffer*.

BACKGROUND

Bovidae (Cetartiodactyla, Ruminantia) is the most diverse family of terrestrial large mammals and makes up the majority of large herbivore species in tropical and subtropical ecosystems across Eurasia and Africa. A recent study of 96 bovid species (Bibi & Tyler 2022) showed that *c.* 10 % of this family's cranial shape diversity (excluding horns) could be explained by a common size-shape allometry. Size was positively correlated with facial elongation, a pattern documented across a wide range of placental mammals (Cardini

2019). In herbivores, selection for both increased size and facial elongation could have promoted repeated diversification into grazing niches, particularly since larger size and longer jaws provide metabolic and mechanical advantages when it comes to the ingestion of grasses, which are often less protein-rich and more abundant in abrasives such as phytoliths and dirt, than herbaceous shrubs or tree leaves (Damuth & Janis 2011; Codron *et al.* 2019).

The largest bovids, past and present, are bovins (tribe Bovini). These include all extant buffalo and oxen, including domestic and wild forms of the genera *Bos* Linnaeus, 1758 (including *Bison* C.H.Smith, 1827), *Bubalus* C.H.Smith, 1827 (including *Anoa* C.H.Smith, 1827), and *Syncerus.* Extant bovins are largely Asian in distribution, and the African buffalo (*Syncerus caffer*) is the only living endemic African bovin. Although commonly called the Cape buffalo, its range extends across much of sub-Saharan Africa, occupying habitats from semi-arid savannas to moist tropical forests, wherever permanent water and grass are available (Prins & Sinclair 2013).

In the Pliocene and Pleistocene, however, African bovins were more diverse. Two or more species often coexisted, distributed among genera such as *Simatherium* Dietrich, 1941, *Pelorovis* Reck, 1928, and *Ugandax* Cooke & Coryndon, 1970. In the late Quaternary, *Sy. caffer* is often found sympatrically with the extinct giant buffalo *Sy. antiquus* (Duvernoy, 1851), which likely survived into the middle Holocene (Gautier & Muzzolini 1991; Gentry 2010). However, the earlier evolution of the clade is not well understood. The oldest fossils attributable to *Syncerus* are known from between 3 Ma and 2.5 Ma, but these are fragmentary and of uncertain species identity (Gentry 1985, 2010; Bibi *et al.* 2017). Their attribution to *Syncerus* is based on horns that are more strongly divergent, inclined, mediolaterally compressed, with a more anteriorly located posterolateral keel, than in its supposed ancestor *Ugandax* (Gentry 2006). A better understanding of the evolutionary origins and development of the *Syncerus* clade has been hindered by a lack of well-preserved material, especially from the 3-2 Ma time interval.

Extant *Sy. caffer* is also notable for its exceptional phenotypic variation across its geographic range. Savanna populations include massive individuals (*c.* 500-800 kg) with dark pelage and long horns that sweep downward from thick bases and often form a fused boss. In contrast, forest-dwelling individuals are much smaller (*c.* 250-320 kg), reddish in color, and bear shorter, simpler horns (Grubb 1972). The stark phenotypic differences among extant African buffalo populations have been attributed to environmental differences, leading to the idea that the various morphs represent ecophenotypes. This ecophenotypic plasticity, expressed across habitats from savanna to forest, provides a modern analog for understanding the developmental flexibility that may also have contributed to morphological diversity in the fossil record. Furthermore, these striking differences exceed the level of ecophenotypic variation typical of other large mammals and have led to a complicated taxonomic history (reviewed below). Heterochrony has been invoked to explain this variation; several authors (Geist 1971; Estes *et al.* 1974; Vrba 1996) emphasized the role of slowed growth (neoteny) in bovid development, while Vrba *et al.* (1994) documented evidence for pedomorphosis along evolutionary allometries in reduncins. Such findings suggest that heterochronic processes may also underlie the disparity observed within *Syncerus*.

Over 50 species names were proposed historically to accommodate this variation (Grubb 2005), but since Lydekker (1913) consensus has generally recognized all African buffalo as a single, highly variable species (reviewed in Grubb 1972). This variability was long suspected to reflect environmental differences, with subspecies interpreted as ecophenotypes. Vrba (1996, 2004) proposed that size differences follow climatic gradients, invoking Bergmann's and Allen's rules: the large-bodied, long-horned savanna morph (*Sy. caffer caffer*) would result from prolonged growth in cooler environments at higher latitudes and altitudes (see also Sinclair 1977).

The pronounced variation among living populations has also led to competing subspecies schemes. Four morphotypes have often been recognized: *Sy. c. caffer* (large, long-horned savanna form of eastern and southern Africa), *Sy. c. nanus* (small, short-horned forest form of central and western Africa), *Sy. c. brachyceros* (intermediate-sized, short-horned savanna form of West Africa), and *Sy. c. aequinoctialis* (large, long-horned savanna form of central Africa) (Grubb 1972; Prins & Sinclair 2013). However, molecular work showed that *Sy. c. nanus*, *Sy. c. aequinoctialis*, and *Sy. c. brachyceros* are not monophyletic, and that the distinctive small "nanus" forest morphotype evolved repeatedly from larger ancestors (Smitz *et al.* 2013). These results supported dividing *Sy. caffer* into two main subclades, *Sy. c. caffer* and *Sy. c. nanus* (the latter including both "aequinoctialis" and "brachyceros"), with all extant buffalo populations descending from a most recent common ancestor dating to *c.* 149-449 ka.

The fossil record contributes little to this recent history. Definite occurrences of *Sy. caffer* before the Late Pleistocene are rare, with only scattered, poorly preserved crania from the Middle Pleistocene (Gentry 2010; occurrences tabulated by Faith *et al.* 2019). By contrast, *Sy. antiquus* is abundant and well documented from the Middle and Late Pleistocene, and even into the Holocene, from southern to northern Africa (Gautier & Muzzolini 1991; Klein 1994). *Syncerus acoelotus* Gentry, 1985 was described from the Early Pleistocene of Olduvai Gorge, and remains confidently recorded only from that site, and from a handful of specimens (Gentry & Gentry 1978). Aside from *Sy. antiquus* and *Sy. acoelotus*, no other extinct species of *Syncerus* have been formally described. Older fossils assigned to the genus remain uncertain: Gentry (1985) attributed material from the Shungura Formation (*c.* 3-2.5 Ma) to *Sy.* ?*acoelotus*, while Bibi *et al.* (2017) referred two *c.* 2.6 Ma specimens from Ledi-Geraru to cf. *Syncerus*. Gentry (2010) later assigned the Shungura material to *Simatherium shungurense* Geraads, 1995, based on a cranium with long, slender, and straight horns. However, we favor Gentry's initial identification of the early Shungura material to *Syncerus*, as explained previously (Bibi *et al.* 2017), and below. Until now, however, the Shungura material remained taxonomically indeterminate, pending discovery of more complete specimens.

The Shungura Formation is a sequence of fossiliferous Plio-Pleistocene deposits, divided into 12 Members (Basal, then A to L, omitting I), dated between *c.* 3.75 Ma and 1.09 Ma. It was first investigated in 1933 by Arambourg (1947), then in 1967-1976 by the International Omo Research Expedition (Arambourg *et al.* 1967; Howell 1968), and since 2006 by the Omo Group Research Expedition (OGRE, Boisserie *et al.* 2008). Stratigraphy and geochronology were described in detail by Heinzelin (1983) and revised by McDougall & Brown (2006, 2008), McDougall *et al.* (2012), and Kidane *et al.* (2014). Most recently Gardin *et al.* (2024, in their supplementary data) integrated all available chronological data to establish an updated age model for the formation.

MATERIAL AND METHODS

Specimens were studied at the Ethiopian Heritage Authority (EHA, formerly Authority for Research and Conservation of Cultural Heritage) at the National Museum of Ethiopia in Addis Ababa, Ethiopia; the National Museums of Kenya in Nairobi, Kenya; and the Museum für Naturkunde in Berlin, Germany. Measurements were taken with standard digital calipers, measuring tape, and angle measure. Horn core lengths were measured using measuring tape along the external (convex) curvature surface. Horn lengths for some extant specimens of *Sy. caffer* were measurable only on the external horn sheath, and horn core length was estimated as 0.64 x sheath length, based on two specimens at the Museum für Naturkunde, Berlin, in which both core and sheath lengths were measurable (and which gave ratios of 0.64 and 0.63). Specimens were classified as adult based on permanent cheek teeth (P2-M3) erupted and in wear, or as immature based on presence of DP-DP4, or if P2-P4 and M3 were still in the process of erupting. All individuals included in this study had M1-M2 already erupted (i.e., no very young individuals were sampled). Individuals of *Sy. caffer* were classified as either "caffer" or "nanus" morphotype based on large size and long horns, or small size and short horns, respectively. Full specimen details are given in a supplementary file (TaxonClassifiers.csv) (Bibi & Boisserie 2025).

Shungura Formation specimen numbers generally take the form of an "OMO" or "L" prefix, followed by locality and specimen numbers. We followed Gentry (1985) in giving the stratigraphic member of Shungura Formation after the specimen number in the text, though this does not form part of the actual specimen number. For example, in "L 444-10005 C", L 444 is the locality, 10005 is the specimen number for that locality (IORE numbering starts at 1, OGRE numbering starts at 10001), and "C" refers to Member C of the Shungura Formation.

Fossil specimens not described below but included in the cranial analyses are KNM–ER 524, GAW-VP-3/210, Atbara 20-88, and NHMUK PV M 34563. KNM–ER 524 is the holotype of *Pelorovis turkanensis* Harris, 1991 and was described by Harris (1991). Specimens GAW-VP-3/210 and Atbara 20-88 are undescribed but have been studied by one of us (F.B.). They are included in this study to provide further taxonomic and chronological context and therefore only a brief description of their provenance is given here. GAW-VP-3/210 derives from the Haradaso Member (*c.* 4.8 Ma, Renne *et al.* 1999) of the Middle Awash study area in Ethiopia (T. White, pers. comm.). It is similar to material of *Ugandax demissum* (Gentry, 1980), initially described as *Simatherium demissum* Gentry, 1980 from Langebaanweg, South Africa, and is attributable to the same species. Atbara 20-88 was collected from Pleistocene deposits at Wadi Turk along the middle Atbara River in eastern Sudan (Abbate *et al.* 2010; Bibi *et al.* personal communication). Luminescence dating at the nearby site of Al Sharafa established a range of *c.* 224-17 ka for the Pleistocene sequences in the area (Tsukamoto *et al.* 2022). Analyses to further constrain the age of the Wadi Turk site are underway (Tsukamoto, Bibi *et al.* personal communication), but for now we assume an age within this timeframe. Atbara 20-88 is much larger than *Sy. caffer*, with horn core bases directed anterolaterally, and is attributable to the extinct giant buffalo, *Sy. antiquus*. NHMUK PV M 34563 is a cast of the holotype of *Homoioceras singae* Bate, 1951 (a synonym of *Sy. antiquus* (Gentry 2010)) described from Singa, Sudan.

These fossil specimens all exhibit differing degrees of diagenetic deformation, including dorsoventral and/or mediolateral compression. However, all retain a high degree of bilateral symmetry. Not all landmarks could be confidently placed on all specimens, Appendix 1 gives the number of missing coordinates per specimen. Sensitivity analyses were conducted to exclude any significant influence of bilateral fossil deformation or missing coordinate estimation on our results. These included a set of analyses with all fossil specimens removed (specimens of *Bos primigenius* Bojanus, 1827 were not considered as fossil for this analysis); one using only the symmetric shape component of the landmark coordinates, which forces bilateral coordinates on the left and right sides of the cranium to be mirrored, artificially removing any bilateral asymmetry; one with landmark coordinates that were missing in more than five specimens deleted; and one with all landmarks which were missing in OMO 53-10001 deleted. Other fossils included in the analysis included six crania of *Bos primigenius* and one of *Bison latifrons* (Harlan, 1825) – however, these are much younger and better preserved than the African fossil specimens. Given its relatively recent extinction, and its survival in the form of domesticated cattle, *Bos primigenius* was not considered a fossil taxon in the sensitivity analyses.

For the 3D geometric morphometric analysis, 43 3D surface models were generated using the Artec Spider and Eva surface scanners, the CREALITY Raptor scanner, from CT scans, or obtained from published or otherwise available datasets (Table 1). Nine models derive from Farke's (2010) dataset (scan data kindly provided by A. Farke), and seven models were obtained from sketchfab.com. We used the same landmark scheme as Bibi & Tyler (2021) and Baird *et al.* (2023), with 53 landmarks chosen to capture cranial shape excluding horns (Fig. 1). These were digitized on each skull using iDAV Landmark Editor v.3.645, Stratovan Checkpoint v.r23.05.30, and Slicer v.5.8.1. All geometric morphometric analyses were conducted in R v.4.5.0 and R Studio v. 2025.05.0+496 (Posit

TABLE 1. — Specimens used in the 3D geometric morphometric analysis. Abbreviations: **AMNH**, American Museum of Natural History, New York; **IMNH**, Idaho Museum of Natural History; **MfN**, Museum für Naturkunde Berlin (previously "Zoological Museum of Berlin", ZMB), mammalian collection; **NHMUK**, Natural History Museum United Kingdom (London). PV refers to the vertebrate paleontology collection; **NME**, Ethiopian Heritage Authority/National Museum of Ethiopia, Addis Ababa. OMO refers to specimens from the Omo Valley. GAW refers to the Gawto beds of the Middle Awash area.

Museum	Specimen	Fossil/ Extant	Abbreviation	Genus	Subgenus	Species
YPM	YPM MAM 9022	Extant	Bo bis	*Bos* Linnaeus, 1758	*Bison* C.H.Smith, 1827	*bison* Linnaeus, 1758
YPM	YPM MAM 9023	Extant	Bo bis	*Bos*	*Bison*	*bison*
IMNH	IMNH R-163	Extant	Bo bis	*Bos*	*Bison*	*bison*
MfN	ZMB Mam 85047	Extant	Bo gau	*Bos*	*Bos*	*gaurus* C.H.Smith, 1827
MfN	ZMB Mam 14802	Extant	Bo gau	*Bos*	*Bos*	*gaurus*
AMNH	M-113755	Extant	Bo jav	*Bos*	*Bos*	*javanicus* d'Alton, 1823
IMNH	IMNH-48001 1770	Fossil	Bo lati	*Bos*	*Bison*	*latifrons* (Harlan, 1825)
MfN	MB Ma 671	Fossil	Bo pri	*Bos*	*Bos*	*primigenius* Bojanus, 1827
MfN	MB Ma 226	Fossil	Bo pri	*Bos*	*Bos*	*primigenius*
NHMUK	NHMUK ARC 1972 5062	Fossil	Bo pri	*Bos*	*Bos*	*primigenius*
NHMUK	NHMUK ARC 1977 5012	Fossil	Bo pri	*Bos*	*Bos*	*primigenius*
NHMUK	NHMUK PV OR 50086	Fossil	Bo pri	*Bos*	*Bos*	*primigenius*
NHMUK	NHMUK ARC 1972 5068	Fossil	Bo pri	*Bos*	*Bos*	*primigenius*
NHMUK	NHMUK 1981_984	Extant	Bo tau	*Bos*	*Bos*	*primigenius*
MfN	ZMB Mam 48424	Extant	Bu arn	*Bubalus* C.H.Smith, 1827	*Bubalus*	*arnee* (Kerr, 1792)
MfN	ZMB Mam 14801	Extant	Bu arn	*Bubalus*	Bubalus	arnee
AMNH	M-152856	Extant	Bu dep	*Bubalus*	*Anoa* C.H.Smith, 1827	*depressicornis* (C.H.Smith, 1827)
AMNH	M-61146	Extant	Bu dep	*Bubalus*	*Anoa*	*depressicornis*
MfN	ZMB Mam 73488	Extant	Bu dep	*Bubalus*	*Anoa*	*depressicornis*
AMNH	M-40046	Extant	Bu min	*Bubalus*	*Bubalus*	*mindorensis* Heude, 1888
AMNH	M-99339	Extant	Bu min	*Bubalus*	Bubalus	*mindorensis*
MfN	ZMB Mam 73510	Extant	Bu min	*Bubalus*	*Bubalus*	*mindorensis*
MfN	ZMB Mam 73496	Extant	Bu qua	*Bubalus*	*Anoa*	*quarlesi* (Ouwens, 1910)
MfN	ZMB Mam 73484	Extant	Bu qua	*Bubalus*	*Anoa*	*quarlesi*
KNM	KNM-ER 524	Fossil	Pe tur	*Pelorovis* Reck, 1928	–	*turkanensis* Harris, 1991
NME	OMO 75/S-1969-2733	Fossil	Si shu	*Simatherium* Dietrich, 1941	–	*shungurense* Geraads, 1995
MfN	Atbara 20-88	Fossil	Sy ant	*Syncerus* Hodgson, 1847	–	*antiquus* (Duvernoy, 1851)
NHMUK	NHMUK PV M 34562	Fossil	Sy ant	*Syncerus*	–	*antiquus*
MfN	ZMB Mam 35750	Extant	Sy caf	*Syncerus*	–	*caffer* (Sparrman, 1779)
YPM	YPM MAM 11649	Extant	Sy caf	*Syncerus*	–	*caffer*
YPM	YPM MAM 9227	Extant	Sy caf	*Syncerus*	–	*caffer*
MfN	ZMB Mam 19143	Extant	Sy caf	*Syncerus*	–	*caffer*
MfN	ZMB Mam 29536	Extant	Sy caf	*Syncerus*	–	*caffer*
MfN	ZMB Mam 35239	Extant	Sy caf	*Syncerus*	–	*caffer*
MfN	ZMB MAM 41820	Extant	Sy caf	*Syncerus*	–	*caffer*
MfN	ZMB Mam 108867	Extant	Sy caf	*Syncerus*	–	*caffer*
MfN	ZMB Mam 108931	Extant	Sy caf	*Syncerus*	–	*caffer*
MfN	ZMB Mam 108991	Extant	Sy caf	*Syncerus*	–	*caffer*
MfN	ZMB Mam 109009	Extant	Sy caf	*Syncerus*	–	*caffer*
MfN	ZMB Mam 41819	Extant	Sy caf	*Syncerus*	–	*caffer*
MfN	ZMB Mam 41818	Extant	Sy caf	*Syncerus*	–	*caffer*
NME	OMO 53-10001	Fossil	Sy n. sp.	*Syncerus*	–	*ekosowan* n. sp.
NME	GAW-VP-3/210	Fossil	Ug dem	*Ugandax* Cooke & Coryndon, 1970	–	*demissum* (Gentry, 1980)

team 2025; R Core Team 2025), mainly using the *geomorph* v.4.0.1 and *RRPP* v.1.0 packages (Collyer & Adams 2018, 2021; Baken *et al.* 2021; Adams *et al.* 2023). Two main sets of analyses were conducted, one including all Bovini, and one including just specimens of *Ugandax* and *Syncerus* species. For each analysis, specimens were Procrustes-transformed to account for rotation, translation, and size differences, and missing landmark coordinates were estimated using the *estimate.missing* function in *geomorph*, with the thin-plate spline option. UPGMA cluster analyses and principal components analyses were conducted on the Procrustes-transformed coordinates. The regression score of shape on size was calculated by projecting the Procrustes-transformed coordinates onto the axis of the shape variables that had the maximum covariation with log centroid size (Drake & Klingenberg 2008; Klingenberg 2016). The regression score was then plotted against centroid size to visually assess the relationship between size, shape, and ontogenetic age (i.e., the allometric trajectories). Tests relied mainly on ANOVA comparisons of the Procrustes-transformed coordinates using the *procD.lm* function in the *geomorph* package. Reference meshes showing the extremes of the first three principal components were made by warping a specimen of *Syncerus caffer* that lay close to the overall mean shape (ZMB Mam 19143) to the maximum and minimum values of each component.

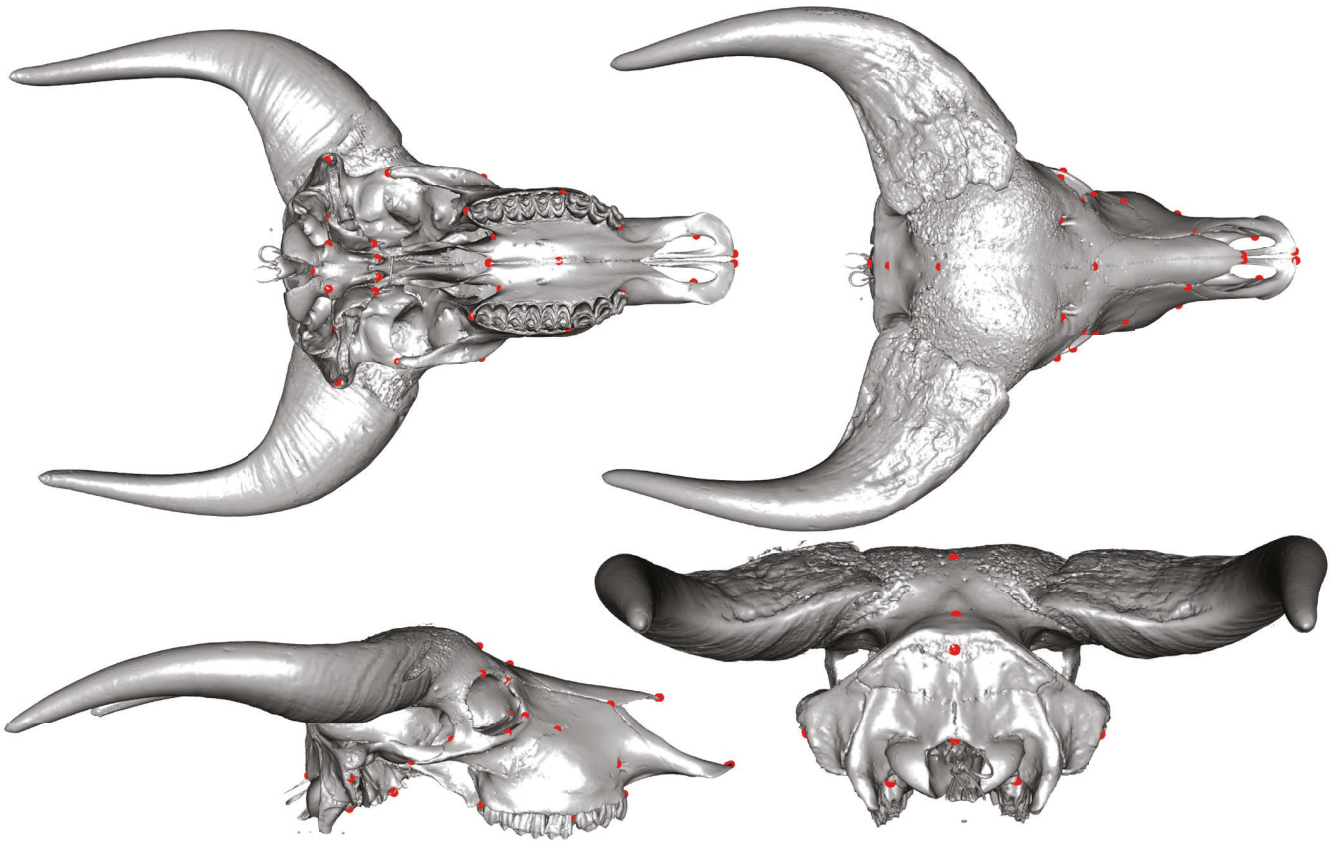

FIG. 1. — Landmark scheme used for the cranial geometric morphometric analysis (following Bibi & Tyler 2021). Specimen shown is *Syncerus caffer* (Sparrman, 1779) ZMB Mam 35239.

All raw data and R scripts to replicate all figures and analyses are provided as supplementary files (Bibi & Boisserie 2025).

Dental size comparisons and plots used measurement data from the Mammal Dental Metrics Database (Bibi 2023), namely deriving from: Lönnberg 1933; Cooke & Coryndon 1970; Churcher 1972; Vrba 1976; Gentry 1980, 1985, 1987; Harris *et al.* 1988; Gentry 1990; Janis 1990; Harris 1991; Harris 2003; Harris *et al.* 2003; Gilbert 2008; Haile-Selassie *et al.* 2009; Everett 2010; Gentry 2011; Faith *et al.* 2015; Rowan *et al.* 2015; Suwa *et al.* 2015; Bibi *et al.* 2017; Faith *et al.* 2020; Rowan *et al.* 2022. Horn core size comparisons and plots used data from: Pomel 1893; Lönnberg 1933; Bate 1951; Gentry 1967, 2006; Gentry & Gentry 1978; Harris 1991; Gilbert 2008; Geraads *et al.* 2012; Bibi *et al.* 2017.

ABBREVIATIONS

AMNH	American Museum of Natural History, New York;
IMNH	Idaho Museum of Natural History;
MfN	Museum für Naturkunde Berlin (previously "Zoological Museum of Berlin", ZMB), mammalian collection;
NHMUK	Natural History Museum United Kingdom (London). PV refers to the vertebrate paleontology collection;
NME	Ethiopian Heritage Authority/National Museum of Ethiopia, Addis Ababa. OMO refers to specimens from the Omo Valley. GAW refers to the Gawto beds of the Middle Awash area.

SYSTEMATIC PALEONTOLOGY

CETARTIODACTYLA Montgelard, Catzeflis & Douzery, 1997
Family BOVIDAE Gray, 1821
Tribe BOVINI Gray, 1821

Genus *Syncerus* Hodgson, 1847

TYPE SPECIES. — *Bos caffer* Sparrman, 1779 by original designation.

GENERIC DIAGNOSIS (MODIFIED FROM GENTRY & GENTRY 1978). — Moderate to large sized bovins with wide skulls and short faces; horn cores emerging just behind the orbits, strongly divergent, short to very long, weakly to greatly compressed dorsoventrally (or mediolaterally), with triangular or subtriangular cross-section, often with keels and weak heteronymous torsion. Characters shared with other bovins: females with horns, basioccipital process short and narrower anteriorly than posteriorly, with large anterior tuberosities, occipital broad and low, becoming broader in later forms by way of increased robusticity of the mastoid region, supraorbital pits quite close together, molars with large basal pillars; lower fourth premolar with paraconid and metaconid growing towards one another or fused. *Syncerus* and *Bubalus* are distinguished from *Bos* (including *Bison*) by horns that emerge just behind the orbits, with keels, flat surfaces, a triangular cross-section, weak curvature, and heteronymous torsion, less hypsodont teeth, and molars with less complicated central cavities and weaker ribs between the styles, and less protruding orbits; but these are probably all

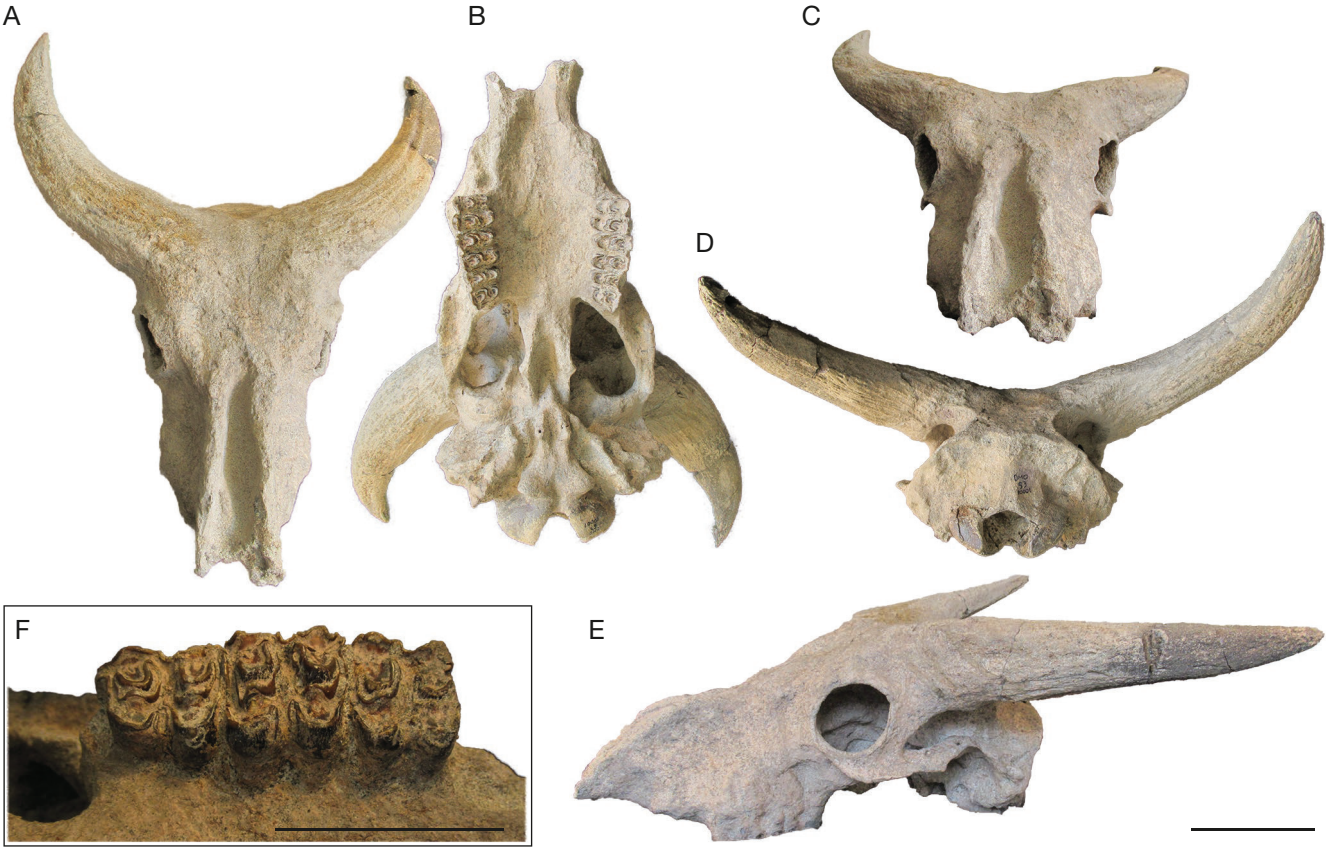

FIG. 2. — Holotype cranium of *Syncerus ekosowan* n. sp. OMO 53-10001: **A**, dorsal; **B**, ventral; **C**, anterior; **D**, posterior; **E**, left lateral; **F**, occlusal views. Scale bars: A-E, 10 cm; F, 5 cm.

plesiomorphic traits in Bovini. Compared to *Ugandax* (from which it likely evolved), *Syncerus* has horns with larger bases, greater divergence, greater dorsoventral (mediolateral) compression, broader and more flattened surfaces (especially the medial or dorsal surface), often with a more triangular basal cross-section, weaker medial/dorsal curvature, and a narrower bulla. Also, in early *Syncerus*, the anterior horn core edge is weakly curved backwards, and the posterior edge is straight, while in *Ugandax* both anterior and posterior edges are either weakly curved backwards (as in the holotypes of *U. coryndonae* Gentry, 2006 and *U. gautieri* Cook & Coryndon, 1970) or relatively straight. Horns of larger species and individuals of *Syncerus* also reach much greater lengths than those of *Ugandax*, which generally do not surpass 400 mm in length. Horns of *Syncerus* are differentiated from those of *Pelorovis* (*P. turkanensis*, *P. oldowayensis* Reck, 1928), which bear no keels, have rounded basal cross-sections, emerge from the back of the cranium and curve strongly anteriorly, and show varying degrees of homonymous torsion. Horns of *Syncerus* are also differentiated from the type and only specimen of '*Pelorovis*' *kaisensis*, a horn core which is much larger, straighter, without keels, and with a rounded cross-section (Geraads & Thomas 1994).

Syncerus ekosowan n. sp.
(Figs 2; 3)

urn:lsid:zoobank.org:act:6971DB10-CE60-4F8F-8451-08EAE386B64F

Syncerus ?acoelotus – Gentry 1985: 139; pl. IV; figs 5-8.

Simatherium shungurense – Gentry 2010: 753.

Likely also: "cf. *Syncerus*" (sic) – Bibi *et al.* 2017: 3.

REFERRED SPECIMENS. — **Holotype. Ethiopia** • OMO 53-10001, an almost complete cranium with both horn cores and right and left M^1-M^3 (Fig. 2; Table 2), housed at the Ethiopian Heritage Authority (National Museum of Ethiopia, Addis Ababa). Discovered by Kampiro Kayrento during OGRE field season 2015. Excavated from Unit C-8 of Member C of the Shungura Formation, with an age of around 2.568 Ma (age model of Gardin *et al.* 2024).

OTHER SPECIMENS. — New specimens: L 193-10027 C-7, right and left horn cores (Fig. 3); L 444-10005 C-9, right and left horn cores, both almost complete (Fig. 3).
Specimens previously described by Gentry (1985) and re-examined for this study: OMO 18-1967-114 C, left horn core; OMO 18-1967-914 C, right horn core; OMO 18-1969-2725 & 2726 C, frontlet with right horn core base (2725) and basal left horn core fragment (2726), same individual; OMO 18/sup-1967-153, 911, and 912 C, left (911-912) and distal right (153) horn cores, attributed to the same individual. Specimens previously described by Gentry (1985) and presumably still at the Natural History Museum in London: L 1-238 B-9/C, juvenile partial cranium with both horn cores, frontals, left orbit, and left upper dP2-M1; L 2-26 B-10, partial cranium; L 16-10 G-4, horn core fragment, side indeterminate (Gentry 1985: pl. III; fig. 1); L 53-3 C, right horn core and partial left horn core; L 147-48a E, fragmentary horn core; L 607-1 G-5, partial cranium; L 744-1 C, right and left horn cores and "fragmentary skull part"; L 837-2 C, right horn core; OMO 23-1967-722 C, right horn core fragment; OMO 58-1968-2316 E/F, left horn core base.

TABLE 2. — Measurements on OMO 53-10001, holotype cranium of *Syncerus ekosowan* n. sp.

Measurements	OMO 53-10001
Horn core DAP x DT	R: 83.2 x 63.4 L: 79.6 x 61.4
Horn core total curved length (along anterior surface)	R: 285 L: 275
Inclination angle of horn core against parietals	45°
Divergence angle of horns	150° in anterior view 120° in dorsal view
Width across dorsal orbits	175
Width across external pedicels	165
Internal distance between horn cores	125
Width between supraorbital foramina	69e
Cranio-facial angle	125°
Parietal-Occipital angle	90° against lateral occipital face 130° against the median nuchal crest
Minimum distance between temporal lines	61.4
Width across mastoids	173 (195 with temporal tubercles)
Occipital height from dorsal foramen magnum	61.1
Occipital height from ventral foramen magnum (basion)	87.6
Width across posterior tuberosities	55.2
Width across anterior tuberosities	27.1
Distance from posterior to anterior tuberosities	53.7
Bulla length	*c.* 34
Upper molar row length	R: 73.7 (70.6 without the metastyle) L: 72.6 (69.1 without the metastyle)

ETYMOLOGY. — From the Nyangatom word for buffalo, in honor of the Nyangatom people who live in the region and have contributed to scientific expeditions to the Shungura Formation over many decades.

TYPE LOCALITY, STRATA, AND AGE. — Ethiopia, Shungura Formation, members B to G, specifically units B-9 or B-10 to G-5 (3.03 or 2.98 to 2.13 Ma; Heinzelin 1983; Gardin *et al.* 2024).

DIAGNOSIS. — A small *Syncerus* about the size of forest populations of extant *Sy. caffer*. Horn cores are short and strongly divergent, emerging from the skull almost horizontally, dorsoventrally compressed, and curving backwards weakly to moderately. The horn core basal cross-section is triangular with two to three keels, and a flattened anterior surface (Fig. 4). The posterior keel is usually the best defined followed by the anterior keel, while the ventral keel (homologous with posterolateral keel in bovids with less divergent horns) is much more rounded, and is located almost as far anteriorly as the anterior keel. Pedicels are not swollen, and the anterior keel does not continue anteriorly along the pedicel as in *Ugandax*. Rugosities continue a short way onto the dorsal surface of the frontal medial to the horn core, indicative of some medial extension of the horn sheath (perhaps incipient horn bossing). Frontal sinuses are expanded and hollow out the pedicel but do not extend into the horn core beyond the very base (like *Ugandax* and unlike *Sy. caffer*). Occipital is broad and low, with a rounded dorsal outline, as in *Ugandax*, with less robust and laterally protruding mastoid regions than in *Sy. caffer*. Temporal lines are moderately spaced apart. Basioccipital is long (longer than in *Sy. caffer*), with prominent anterior tuberosities that are much closer together than the posterior ones. Bulla is medium sized and strongly compressed mediolaterally (as in *Sy. caffer*, and unlike the enlarged bullae in *Ugandax*). A large, laterally projecting tubercle is present above the acoustic meatus. Tooth row located more anteriorly than in *Sy. caffer*, but like *Ugandax* (with posterior border of the M3 located beneath the anterior orbital orbit). The lateral palatal indentations reach the level of the posterior M3 and are slightly further anterior than the median one. In many ways this is a species slightly more derived than *U. coryndonae*, but more primitive than later *Syncerus* like *Sy. caffer* and *Sy. antiquus* and perhaps also *Sy. acoelotus*. Further differences from these species are given below.

DESCRIPTION

The holotype cranium OMO 53-10001 (Fig. 2) is the most complete specimen known of an early *Syncerus*. Horn cores arise just behind the orbit, are strongly inclined (45° against the parietals) and strongly divergent (150° in anterior view, and 120° in dorsal view), arising almost straight sideways and curving backwards (homologous to the medial curvature in more upright horns such as those of *Ugandax*). They are of moderate length, about two-thirds the total length of the cranium. Cross-section is triangular with three keels, posterior keel is quite sharp, and the anterior (anterodorsal) keel is rounded but well defined. The posterolateral (ventral) keel is the least well defined and quite rounded. It is located almost as far anteriorly as the anterior keel, which results in a flat anterior surface to the horn core. The medial (dorsal) and posterolateral (ventral) surfaces are also quite flat, but less so than the anterior surface. Horns are mediolaterally (dorsoventrally) compressed. Wide longitudinal grooves cover the horn core and are most regularly expressed on the dorsal and anterior surfaces. The anterior keel continues ventrally as a rugosity onto the frontal, and there are weak rugosities on the pedicel and frontal medial and anterior to the horn core, indicative of the extension of the horn sheath onto the frontal bones as in extant *Syncerus*. Torsion is basically absent, though there is a hint (perhaps 10° from base to tip) of heteronymous torsion on the right horn core especially.

Features of the cranium are common to most bovins, especially of the buffalo group (Bubalina) and extant *Syncerus*: dorsal braincase at the parietals is flat; temporal fossae are well developed below the horn cores and to either side of the braincase; temporal lines remain wide apart, at their closest still being wider than the foramen magnum. Also common to extant *Sy. caffer* and probably also Pleistocene African bovins, there is a very large tubercle projecting laterally just dorsal to the auditory meatus. The occipital surface is low and wide in outline, quite flat, with extremely narrow and sharp nuchal ridge (dorsal border). The basioccipital is long; posterior tuberosities are very prominent, anterior tuberosities less prominent and much closer together than posterior ones. The bulla is strongly compressed mediolaterally, with a wide space between it and the posterior tuberosities of the basioccipital (similar to many bovins, but not to *Si. shungurense* or *Ug. coryndonae*, which have wide bullae). The zygomatic has an extremely prominent, ventrally

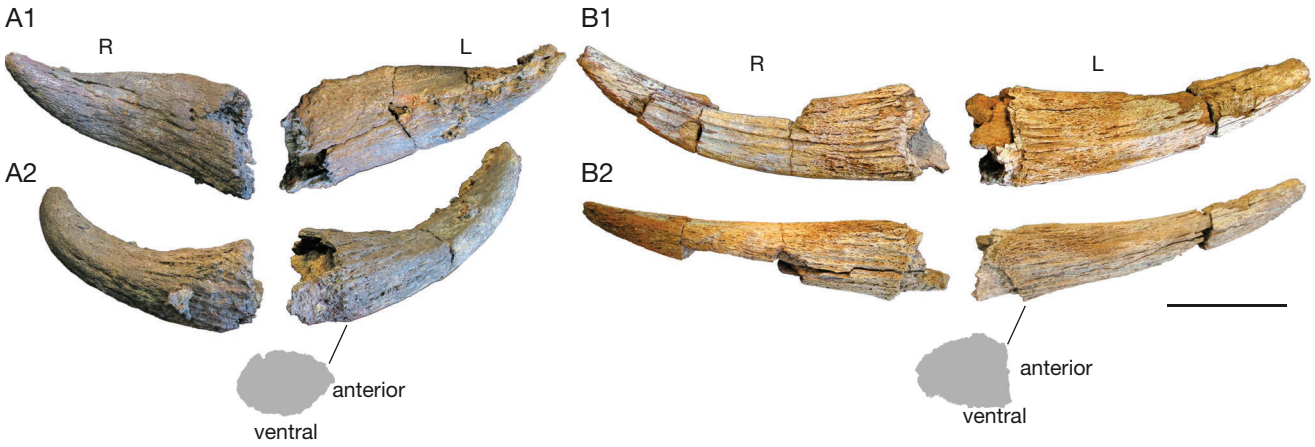

FIG. 3. — Horn cores referred to *Syncerus ekosowan* n. sp. : **A**, L 193-10027; **B**, L 444-10005. Both are right (**R**) and left (**L**) horn cores shown in dorsal (**A1**, **B1**) and anterior (**A2**, **B2**) views. Basal cross-sections shown as if looking into the horn core from the base. Scale bar: 10 cm.

projecting masseteric ridge and deep masseteric fossa on its ventral surface, extending onto the posterior maxilla. The zygomatic bar is very narrow at its anterior end below the anterior orbit. The anterior edge of the orbit is located above the posterior edge of the M^3. The lateral palatal indentations reach the level of the posterior edge of M3, while the median indentation is located slightly more posteriorly. The cranium preserves left and right first to third molars only, and these are in quite advanced wear (late middle to early late wear). As expected for Bovini, these have rounded lingual cusps with large basal pillars, labial cusps with prominent styles and ribs, complexly shaped internal enamel cavities, small oval central enamel islands. The M3 has a tall and prominent metastyle. Lengths of the right and left upper molar rows are 74.3 and 72.8 mm respectively.

The remaining assigned horn cores match those of the cranium in their basal size and length, weak posterior curvature, triangular cross-section, mediolateral (dorsoventral) compression (though this is weaker in most specimens than in the type), flattened surfaces and three more or less-defined keels. As previously described (Gentry & Gentry 1978; Gentry 1985) for both the Shungura *Syncerus* and for Olduvai *Sy. acoelotus*, the frontal sinuses only reach into the very base of the horn core and no further. The pedicel is hollowed into a single open chamber without bony struts (similar to the alcelaphin condition and unlike extant bovins).

Two specimens show significant variation. The OMO 18-1969-2725 & 2726 horn cores (same individual) differ in having an ovate to diamond cross-section, whereby even the dorsal surface is rounded (Fig. 4). Furthermore, there is no indication of a posterolateral keel, and their dorsoventral compression is much greater. However, the cross-section is still wider anteriorly than posteriorly, and the divergence, surface texture, and basal rugosities of the horn cores, and the overall size, frontal morphology, and limited extent of the frontal sinuses all match the other specimens of *Syncerus ekosowan* n. sp. The basal horn core anteroposterior diameter (and probably also length) is of similar size, frontals are thick, and the interfrontal and frontoparietal sutures all indicate an adult individual. L 193-10027 is a pair of short horn cores that differ from all other specimens referred here in having pronounced torsion and strong dorsally directed curvature. What is interesting is that the torsion is homonymous, entirely opposite to the condition in buffaloes (Bubalina), or even the Bovinae in general (Bovini, Tragelaphini, Boselaphini). Homonymous horn torsion is normally characteristic of bison and oxen (Bovina, *Bos* including *Bison*). L 193-10027 also lacks keels, and the horn core cross-section is ovate, with a narrower posterior end and wider anterior end. L 193-10027 resembles the short-horned crania attributed to *Syncerus* sp. and *Sy. acoelotus* from Daka, Middle Awash (Gilbert 2008) and Olduvai (Gentry & Gentry 1978: pl. 4; fig. 2). These are further discussed below. It is possible that OMO 18-1969-2725 & 2726 and L 193-10027, with their weaker keels and more ovate cross-sections, represent female individuals.

Gentry (1985) gave the length of three horn cores, L 837-2, L 1-238 B, and L 744-1, as *c.* 200 mm, *c.* 210 mm, and 240 mm, respectively. This is shorter than the 275-320 mm range measured on the OGRE and IORE specimens described here. L 837-2 and L 1-238 B are on the smaller end of referred specimens in terms of basal dimensions. The partial cranium L1-238 B appears to be slightly larger in overall size than OMO 53-10001, but with smaller and shorter horns. Occipital regions in partial crania L 2-26 B and L 607-1 G are also of similar to slightly larger size than in OMO 53-10001.

While there is abundant isolated dental material attributable to Bovini from the Shungura Formation, it is difficult to distinguish among different, similarly sized species, such as *Sy. ekosowan* n. sp. and *Ug. coryndonae*, or possibly even smaller individuals of *Si. shungurense*. Therefore, the only dental material attributed with confidence to *Sy. ekosowan* n. sp. are for the moment just the teeth attached to the holotype cranium. Similarly, postcranial remains – even when these are collected – are very difficult to assign to species with confidence, and for the time being are not considered here. Further work may refine the situation.

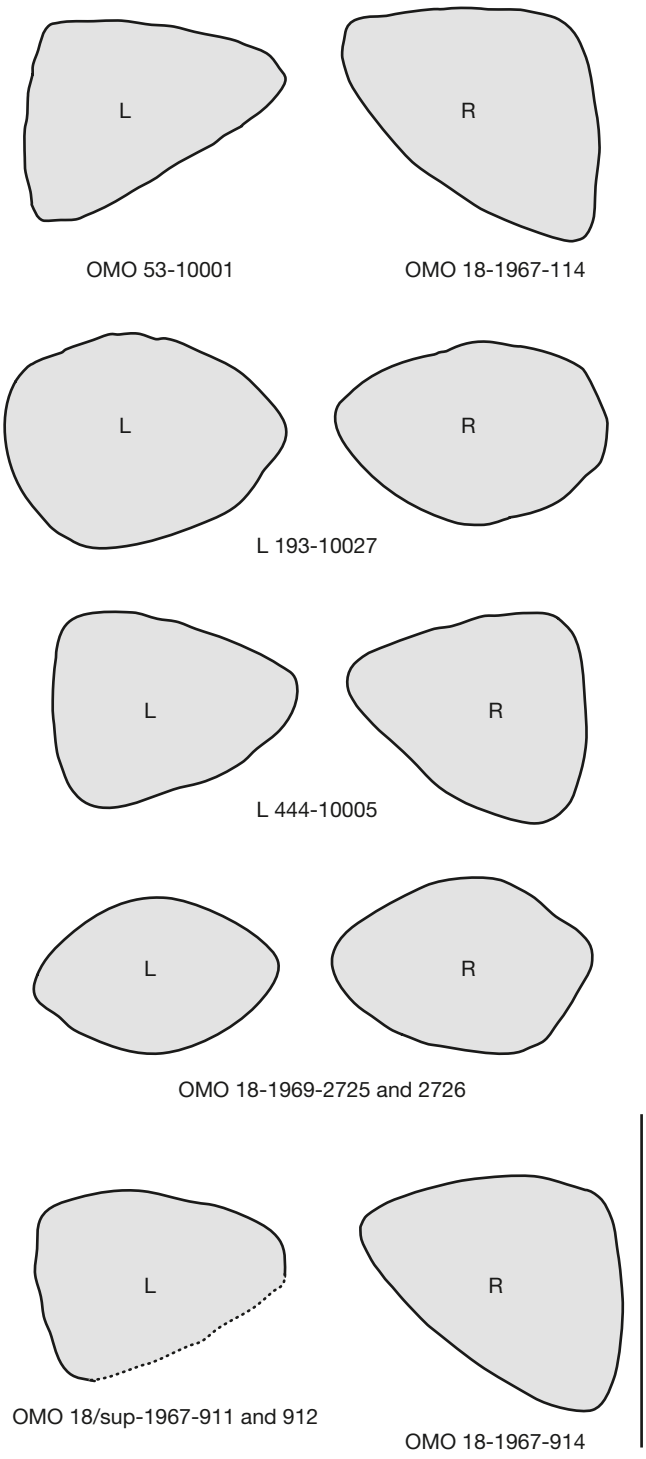

Fig. 4. — Basal cross-sections of horn cores of *Syncerus ekosowan* n. sp. All shown in distal view (as if looking into the cranium). Dorsal is to the top, ventral to the bottom, anterior to the sides, and posterior to the midline of the figure. Abbreviations: **L**, left; **R**, right. Scale bar: 10 cm.

Comparisons

Syncerus ekosowan n. sp. differs from *Ugandax coryndonae*, best known from Late Pliocene deposits at Hadar (Gentry 2006; Geraads *et al.* 2012), by its smaller size, horn cores with greater divergence, greater mediolateral (dorsoventral) compression (Fig. 5A), stronger curvature, and more forward location of the posterolateral keel resulting in a flattened anterior surface. These horn features also generally characterize the genus *Syncerus*, being more or less common to all later species, i.e., *Sy. acoelotus*, *Sy. antiquus*, and *Sy. caffer*. However, horns of *Sy. ekosowan* n. sp. and *U. coryndonae* both show a large range of variation, and isolated horn cores might in some cases be difficult to distinguish. In *Ugandax*, the anterior pedicels are swollen, but not in *Syncerus*. In *Ugandax* the anterior keel continues down the pedicel as a discrete linear rugosity, while in *Syncerus* any pedicel or frontal rugosities are less well defined and, while best developed anteriorly, are present medial to the horn core (possibly reflecting incipient horn sheath bossing). Supraorbital foramina in *Ugandax* are associated with shallow round or elongated depressions (pits or grooves), while these depressions appear absent in OMO 53-10001, though the frontal surface is not well preserved. The basioccipital is very similar in proportions, but OMO 53-10001 has larger anterior tuberosities than generally observed in specimens of *U. coryndonae*. The Hadar *Ugandax* has very large bullae (Gentry 2006 referred to these as "moderately large"), while in OMO 53-1000 these are smaller and more mediolaterally-compressed, and more similar to the condition in extant Bovini.

Simatherium shungurense was described based on a cranium from Member G of the Shungura Formation (holotype: OMO 75/s-1969-2924 G; Geraads 1995) and other crania almost certainly attributable to the same species are known from the Middle Awash and Koobi Fora (discussed by Bibi 2009). *Syncerus ekosowan* n. sp. differs from *Si. shungurense* in much shorter horns (Fig. 6) that are much more divergent. In *Si. shungurense*, the horn cores are much longer, more slender, quite straight, arising above or just behind the orbits, strongly inclined posteriorly, and only weakly divergent. Cranial metrics of *Si. shungurense* are mostly larger than in OMO 53-10001 (e.g., upper molar length of 88 mm compared to *c.* 73 mm, respectively). In *Si. shungurense* the basioccipital tuberosities are not very prominent, and project less than in the smaller OMO 53-10001 cranium. *Simatherium shungurense* also has very wide auditory bullae that almost contact the posterior tuberosities, in contrast to the Shungura (and extant) *Syncerus*, in which the bullae are compressed mediolaterally, with a large space between them and the posterior tuberosities. In *Si. shungurense* the lateral palatal indentations are placed far posterior to the M^3, and level with the median indentation, while in OMO 53-10001 they are slightly anterior to the median indentation. The slenderness of the horns in *Si. shungurense* led Gentry (2010) to suspect that it might have been a female, and he further proposed that the Shungura *Syncerus* might be attributable to *Si. shungurense* instead (and specifically that the horn core L 16-10 G could belong to a male *Si. shungurense*). However, fundamental differences in size, as well as in the shape, length, and orientation of the horns between *Sy. ekosowan* n. sp. (possibly including L 16-10 G, though we were not able to examine this specimen) and *Si. shungurense* cannot be explained by sexual dimorphism. Similarly, the differences between *Si. shungurense* and *Pelorovis* spp., and *Sy. acoelotus* are too great to permit explanation by sexual dimorphism.

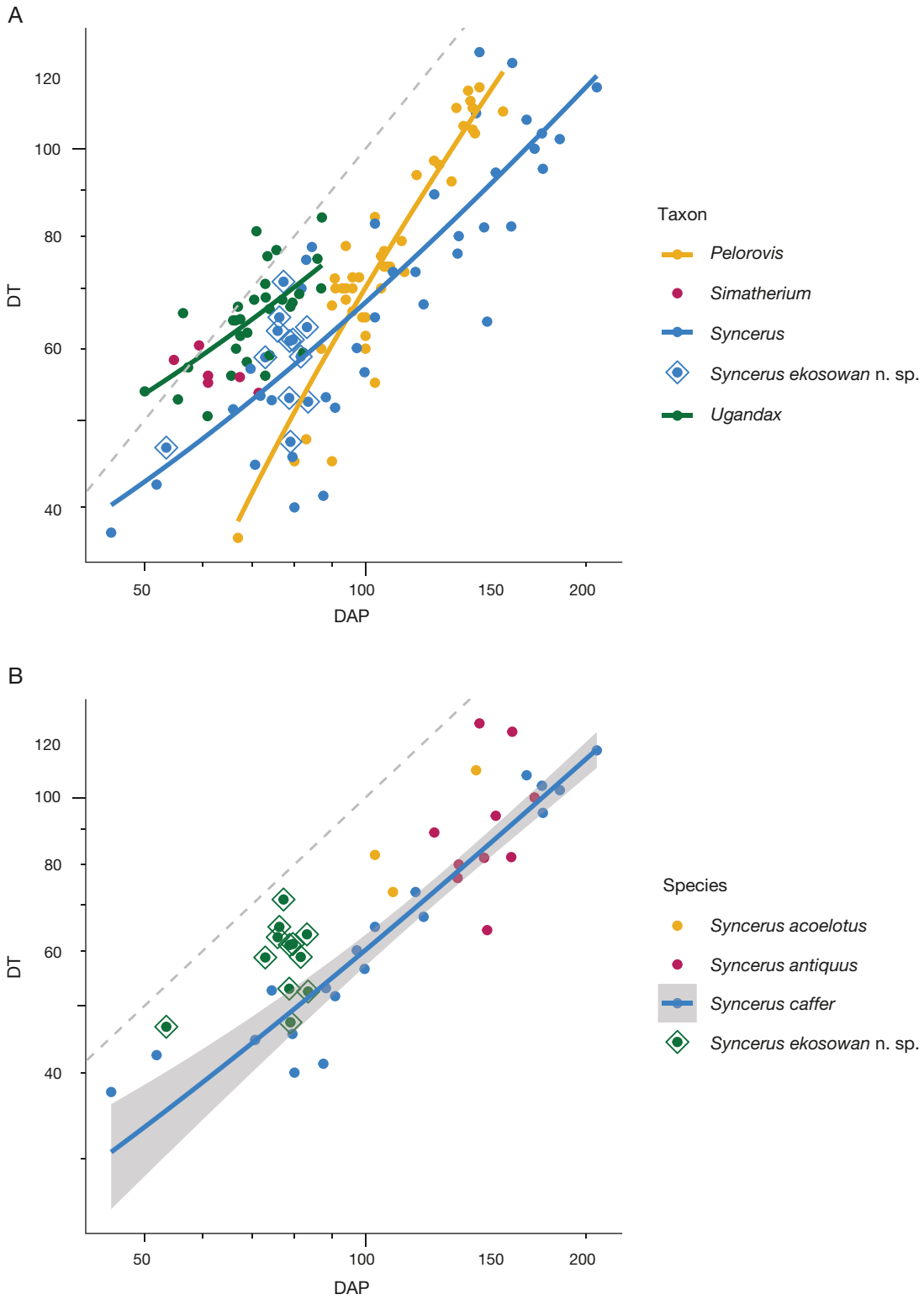

FIG. 5. — Basal horn core anteroposterior (**DAP**) and transverse (**DT**, dorso-ventral in *Syncerus* Hodgson, 1847) diameters in: **A**, African fossil and extant bovins; **B**, *Syncerus* spp. The **dashed line** is the 1:1 line (i.e., no horn core compression). *Ugandax* Cooke & Coryndon, 1970 shows the least transverse compression. *Pelorovis* Reck, 1928 and *Syncerus* have different size-shape allometries: in *Pelorovis*, small specimens exhibit greater transverse compression than larger specimens, while the opposite is true in *Syncerus*. Within *Syncerus*, *Sy. caffer* (Sparrman, 1779) exhibits the greatest degree of transverse compression. Specimens of *Syncerus ekosowan* n. sp. (**diamonds**) overlap with both *Ugandax* and *Sy. caffer* in compression. Units are in mm. Axes are log-scaled.

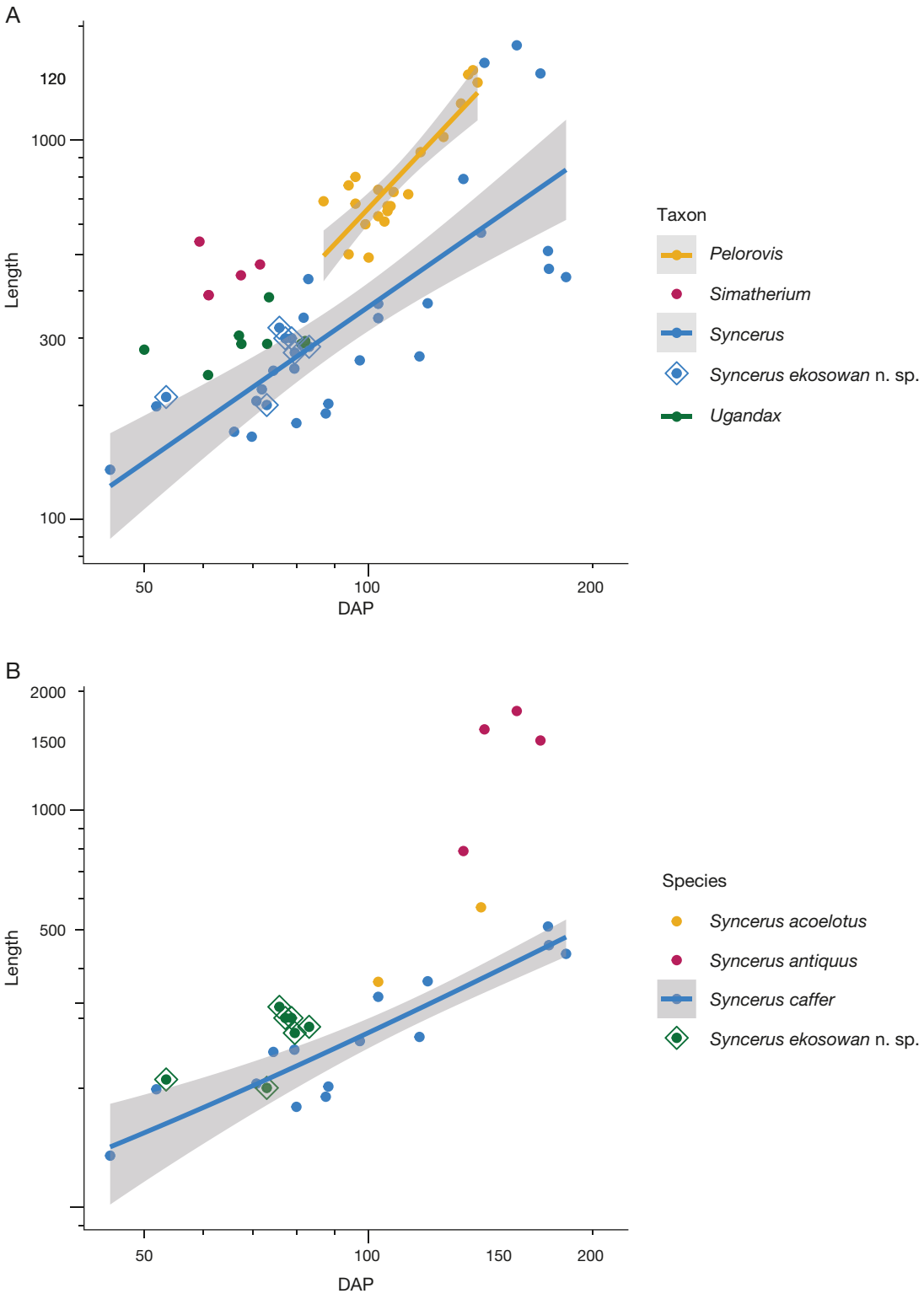

FIG. 6. — Horn core length plotted against basal anteroposterior diameter (**DAP**) in: **A**, Bovini; and **B**, *Syncerus* spp. *Syncerus caffer* (Sparrman, 1779) horns are relatively short for their basal size. Relative horn length in *Sy. ekosowan* n. sp. (**diamonds**) is intermediate between *Ugandax* Cooke & Coryndon, 1970 and *Sy. caffer*. Horn length in *Sy. antiquus* (Duvernoy, 1851) is much greater than predicted by the length to basal size relationship in other species of *Syncerus* Hodgson, 1847. Units are in mm. Axes are log-scaled.

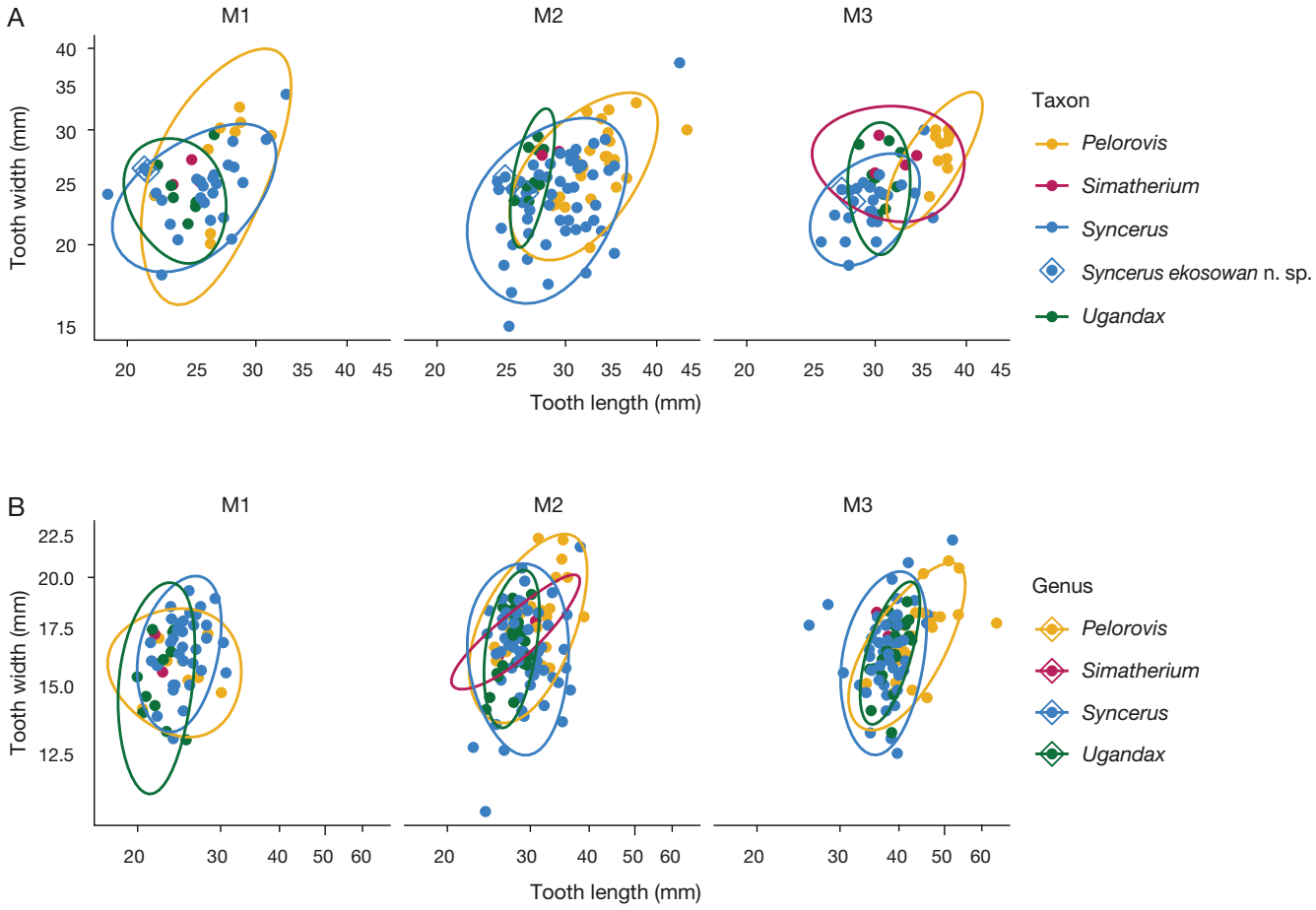

Fig. 7. — Molar length and width in African bovins (fossil and extant). The only teeth attributable with confidence to *Syncerus ekosowan* n. sp. are those on the holotype cranium OMO 53-10001 (i.e., uppers) and these are similar in size to small specimens of *Syncerus* Hodgson, 1847. Teeth of *Syncerus* are similar in size to those of *Ugandax* Cooke & Coryndon, 1970, but smaller than those of *Pelorovis* Reck, 1928, though overlap is high. Teeth of OMO 53-10001 (plotted with **diamond outlines**) are wide in relation to their length, but it is not certain that this is common to all *Sy. ekosowan* n. sp. Note x and y axes are log-scaled.

Syncerus ekosowan n. sp. differs from the holotype of *Sy. acoelotus* (a calvarium with horns from Upper Bed II in Olduvai Gorge, Gentry & Gentry 1978) in smaller size, horn cores that are shorter, less divergent, and with a more triangular cross-section (Fig. 6). The lack of penetration of the horn core by the frontal sinuses is common to both. Gentry & Gentry (1978: pl. 4; fig. 2) also attributed a shorter-horned specimen to *Sy. acoelotus*, and another specimen was later described by Gilbert (2008: fig. 3.15) from the Daka Member in the Middle Awash (*c.* 1 Ma). The Daka specimen, BOU-VP-1/36, is large and heavy-set, with horns that are short, strongly compressed mediolaterally (dorsoventrally), and oval in cross-section, with strong medial curvature. Some specimens of *Sy. ekosowan* n. sp. (e.g., L 139-10027, OMO 18-1969-2725) resemble these shorter-horned forms in their more ovate cross-sections, but differ in being longer, in having much larger bases with more triangular cross-sections, and stronger posterior curvature. Furthermore, the Daka cranium, despite having smaller horns, is much larger in size than *Sy. ekosowan* n. sp., with broader frontals and parietals that are flattened and almost in the same plane, an occipital surface that is much wider, with a long and horizontal dorsal border, and an extremely enlarged mastoid region. These features suggest that the Daka short-horned *Syncerus*, and likely the Olduvai specimen too, might be subadult individuals of large species such as *Sy. acoelotus* or *Sy. antiquus*. The consistency of the morphology across the assemblage of *Syncerus ekosowan* n. sp., which spans members C to G of the Shungura Formation, and the lack of a greater variation of lengths, shapes, and sizes in the fossil record argues against the possibility of *Sy. ekosowan* n. sp. being an eco-phenotypic variant of another highly variable species. It differs significantly from all its contemporaries or near-contemporaries (*Si. shungurense*, *U. coryndonae*, *Sy. acoelotus*), and the fossil record includes no intermediate forms that could bridge the morphological differences between *Sy. ekosowan* n. sp. and any of the other species.

Syncerus ekosowan n. sp. differs from all varieties of extant *Sy. caffer* in that the frontals between the horn cores are not raised into a broad ridge (intercornual torus, even present in diminutive forest buffalo individuals), in having a taller (less wide) occipital surface, and a longer basioccipital; in a palate that is located slightly more anteriorly (with the posterior edge of the M3 located below the anterior orbit, while it is below the central orbit in *Sy. caffer*); in frontal

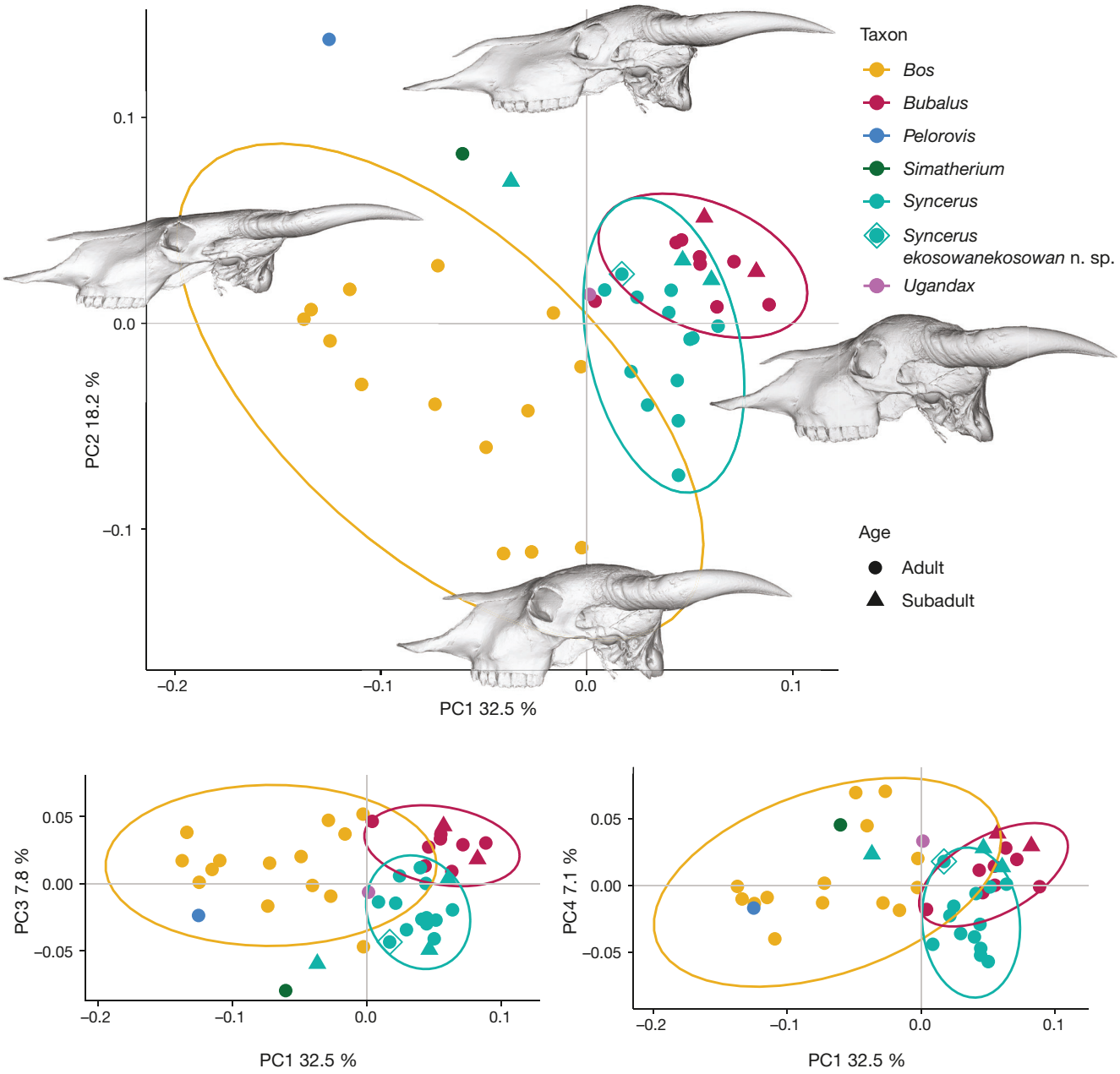

FIG. 8. — The first four principal components of cranial shape in Bovini, with 95 % ellipses. Percentages indicate the amount of variation explained by each component. *Bubalus* C.H.Smith, 1827, *Syncerus* Hodgson, 1847 + *Ugandax* Cooke & Coryndon, 1970, and *Bos* Linnaeus, 1758 (including *Bison* C.H.Smith, 1827) are best differentiated along the first principal component (**PC1**). OMO 53-10001 (shown with **diamonds**) plots with other *Syncerus* specimens. Note the shape analysis considered the cranium only, without horns. See Appendix 3 for version with taxon labels.

sinuses that are less extensive only reaching the basal horn core, while these extend deep into the horn core, the posterior frontals, parietals, and possibly even the occipitals in some individuals of *Sy. caffer* (Farke 2010). Most or all these features in OMO 53-10001 are also shared with *Ug. coryndonae*, suggesting they are all plesiomorphic for the lineage. OMO 53-10001 further differs from the larger (i.e., savanna) individuals of *Sy. caffer* in much smaller size, smaller, shorter, and less divergent horn cores that are less dorsoventrally compressed above the base and lack expanded bases and bossing (Figs 5; 6). It is of similar to slightly smaller size as small, forest-dwelling individuals (*Sy. caffer* '*nanus*'), but has horns that are relatively much larger, located less far back on the cranium, more divergent and less posteriorly directed, less inclined and remaining above the level of the dorsal cranium (dropping below in *Sy. c. nanus*), with a much better developed triangular cross-section and weaker mediolateral (dorsoventral) compression, and less evidence of a frontal boss.

Dental differences are difficult to identify since only the holotype preserves teeth that can be confidently attributed to the new species. Compared to other *Syncerus* spp., the

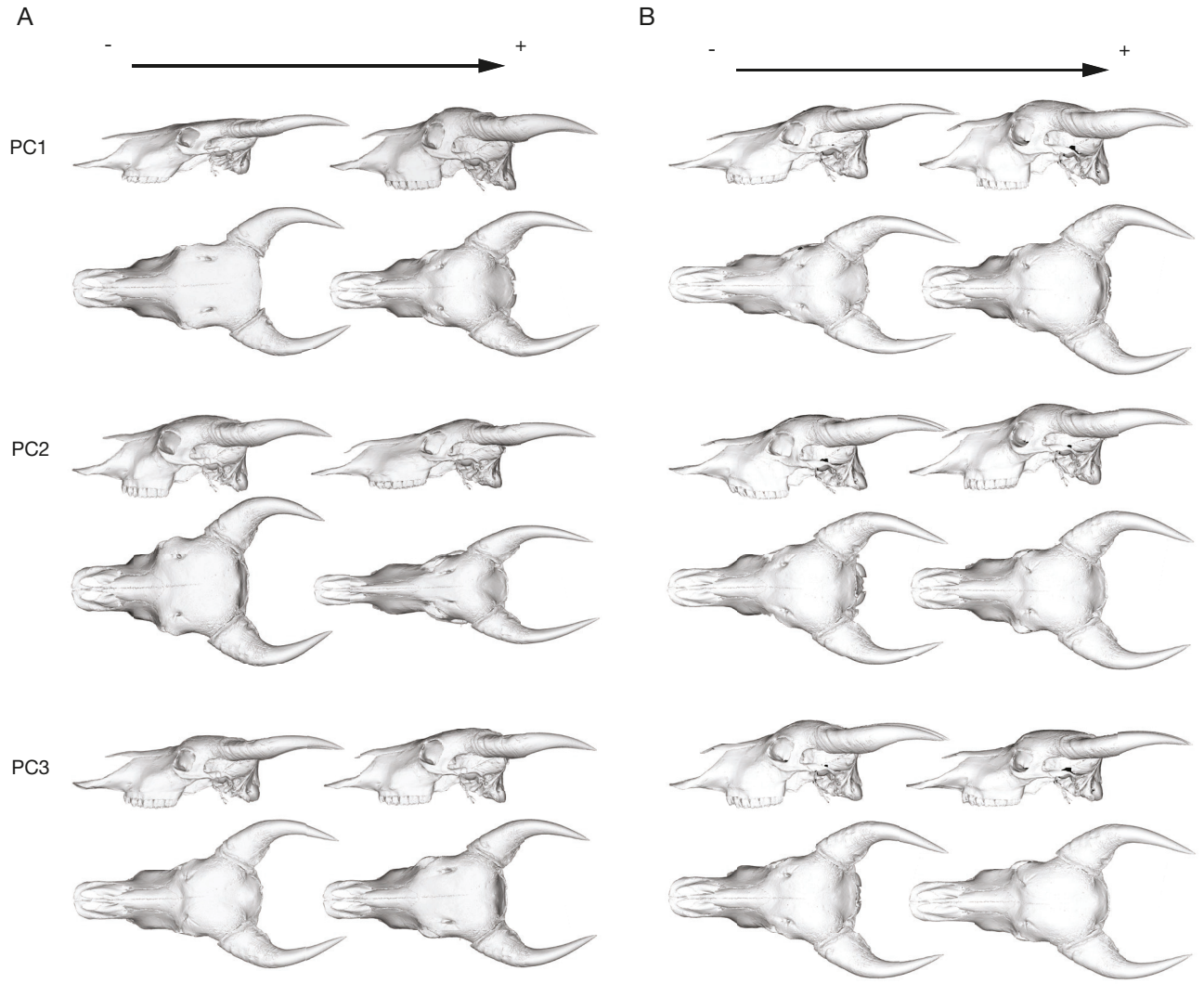

FIG. 9. — Shape changes associated with the first three principal components: **A**, all Bovini; **B**, *Ugandax* Cooke & Coryndon, 1970 and *Syncerus* spp. Crania made by warping a mesh of *Syncerus* Hodgson, 1847 caffer located closest to the total sample mean shape. Note the shape analysis considered the cranium only, without horns. See Appendix 8 for version with fossils removed prior to the analysis.

upper molars in OMO 53-10001 are small and wide relative to their length (Fig. 7). They differ from those of *Sy. caffer* in smaller size and possibly in having less prominent labial ribs and basal pillars and lower-crowned teeth. Lengths of the right and left upper molar rows are comparable to the smallest individuals of extant *S. caffer nanus*, and similar in size to a maxilla of *Syncerus acoelotus* from Olduvai (Gentry & Gentry 1978). An estimate of premolar length on the missing upper premolars of OMO 53-10001 is *c.* 45-55 mm, giving a premolar to molar length ratio of *c.* 65-70 %, which is similar to that in extant individuals of *Sy. caffer* (59-70 %, n = 17, supplementary data). Although no lower dentitions can be attributed confidently to *Sy. ekosowan* n. sp., a large number are known from the Shungura Formation, and these differ from extant *Sy. caffer* in longer premolar rows; Gentry (1985) reported a lower premolar to molar length ratio of 66 % for a Shungura mandible and a range of 55-62 % for six mandibles of *Sy. caffer*. Furthermore, lower fourth premolars retain the plesiomorphic condition of posteriorly slanted metaconids and open anterior lingual valleys, while in *S. caffer*, the metaconid is anteriorly expanded and the anterior lingual valley is closed (Gentry 1985; Bibi personal communication).

GEOMETRIC MORPHOMETRICS

ANALYSIS OF BOVINI

In the UPGMA cluster dendrogram (Appendix 2), *P. turkanensis* was strongly differentiated from all other bovins, Bubalina and Bovina were distinguished from each other (although not consistently), and all fossil specimens besides *Pelorovis* grouped together in a position closer to Bubalina than to Bovina. The cluster results only provide general confirmation of the resemblance of the cranium

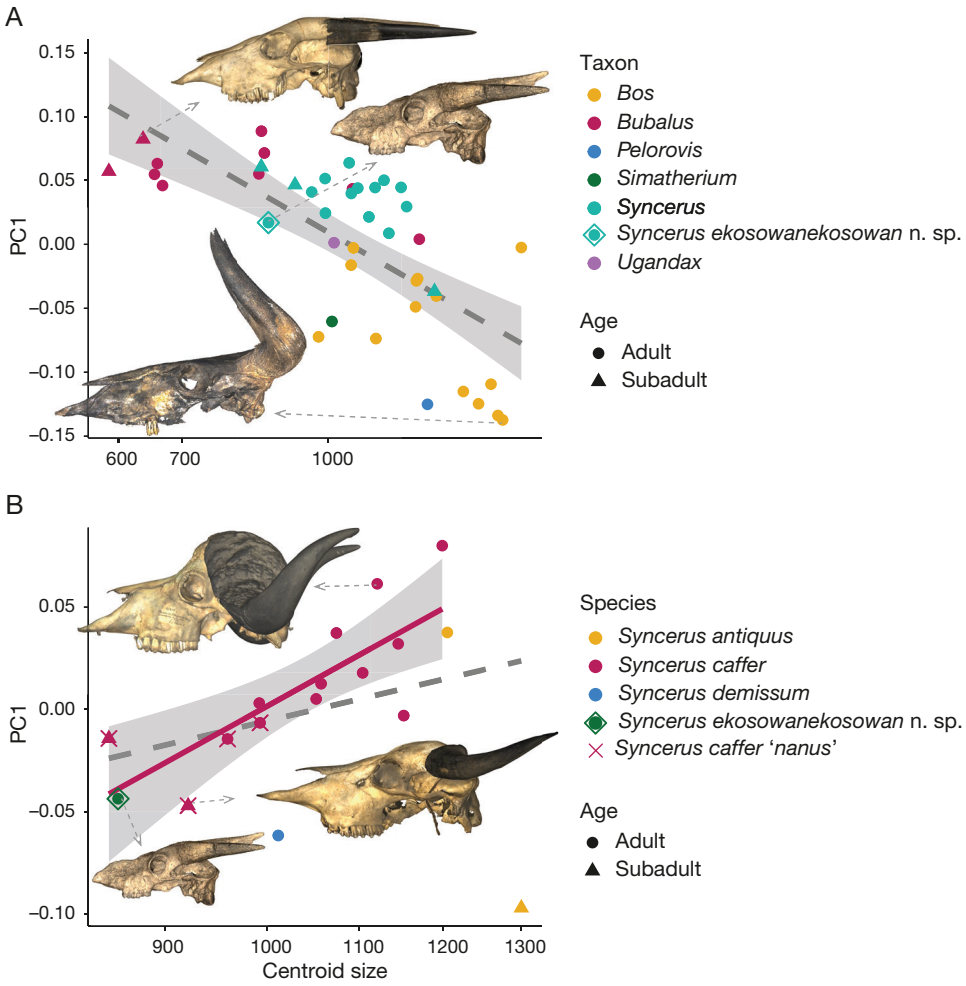

Fig. 10. — The first principal component (**PC1**) plotted against centroid size: **A**, all specimens (Bovini); **B**, *Syncerus* Hodgson, 1847 and *Ugandax* Cooke & Coryndon, 1970 only. In **A**, bovins show increasing facial elongation and gracilization (more positive PC1 values) with increasing size. The relationship is not significant within any of the three extant genera. In **B**, *Syncerus* shows the opposite relationship, through the amount of change is much smaller. Note that one specimen of *Sy. antiquus* (Duvernoy, 1851) is an extreme outlier (**bottom right**). **Dashed line** is the fit for all data points. **Solid line** in **B** is the fit for *Sy. caffer* (Sparrman, 1779) only. X-axes are log-scaled. See Appendix 9 for version with taxon and specimen labels and Appendix 10 for version with fossils removed prior to the analysis.

of *Sy. ekosowan* n. sp. OMO 53-10001 to both Asian and African buffaloes. Analyses of the Procrustes-transformed shape coordinates indicate that genera differ significantly in shape (Procrustes ANOVA, $p = 0.001$, $Z = 7.1$). Cranial shape differences among *Bos*, *Syncerus*, and *Bubalus* are all significant (Pairwise Procrustes ANOVA, $p < 0.05$, $Z > 2.1$). Pairwise comparisons among genera were all significant, except for the comparison of *Pelorovis* and *Simatherium*, and all comparisons against *Ugandax*. However, all three of these fossil genera are represented here by a single specimen each, so these results might reflect low statistical power, rather than an actual lack of shape differences.

Among Bovini, the first four principal components of cranial shape explained 32 %, 19 %, 8 %, and 6 % of the variation, respectively (Figs 8; Appendix 3). Cranial shape changes associated with the first three components are shown in Figure 9A. Bubalina and Bovina separate along first principal component (PC1), with dorsoventrally deeper crania, shorter faces, less protruding orbits, and more anteriorly located horns in the Bubalina (Figs 8; 9). PC1 is strongly correlated negatively with log centroid size (Spearman's rank correlation test, $p < 0.001$, rho = –0.76, $R^2 = 0.58$), with larger individuals exhibiting more elongated faces (Fig. 10A). This relationship is however not significant within any of the three extant genera (*Bos*, *Syncerus*, *Bubualus*, $p > 0.05$). *Bos* displays much higher disparity than *Syncerus* and *Bubalus*, exemplified by the large differences between *Bos primigenius* and bison species along PC2, with deeper and broader crania, shorter faces, and more protruding orbits in bison (Appendix 3). The holotype of *Sy. ekosowan* n. sp., OMO 53-10001, consistently groups close to other specimens of *Syncerus*. *Pelorovis turkanensis*, *Si. shungurense,* and *Sy. antiquus* are located at the positive ends of both PC2 and PC3, reflecting crania that are narrow in both dorsoventral and medio-lateral dimensions. Sensitivity analyses indicate that the primary

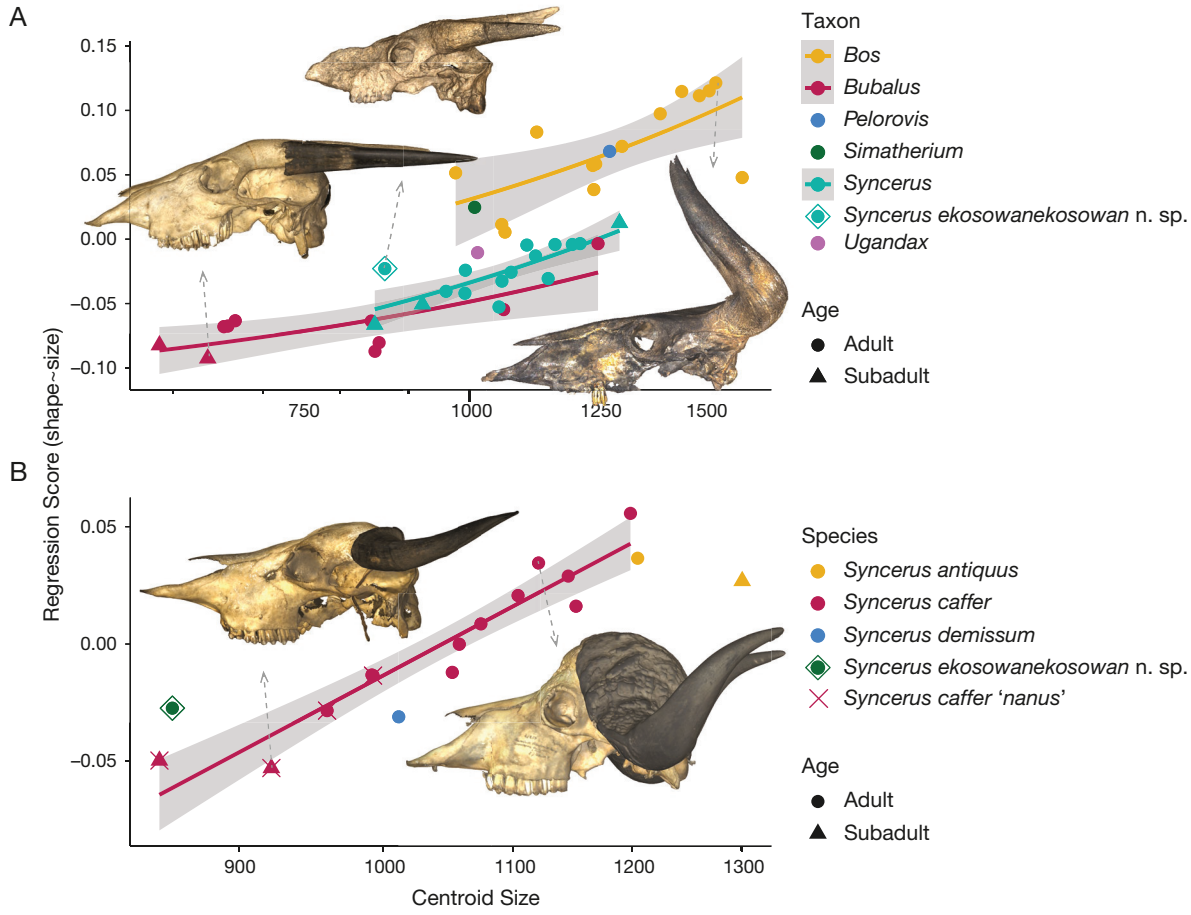

Fig. 11. — The regression score of cranial shape on log centroid size plotted against centroid size: **A**, all specimens (Bovini); **B**, *Syncerus* Hodgson, 1847 and *Ugandax* Cooke & Coryndon, 1970 only. In **A**, the buffaloes (*Bubalus* C.H.Smith, 1827 + *Syncerus* Hodgson, 1847) differ in intercept from oxen (*Bos* Linnaeus, 1758 including *Bison* C.H.Smith, 1827). *Syncerus ekosowan* n. sp. lies closest to the size-shape relationship of subadults and small, short-horned ('nanus') adults of *Syncerus caffer* (Sparrman, 1779). X-axes are log-scaled. See Appendix 11 for version with taxon and specimen labels and Appendix 12 for version with fossils removed prior to the analysis.

shape components identified in the PCA are not strongly affected by deformation or the estimation of missing landmark coordinates (Appendices 4-8; 10; 12).

Among all Bovini, shape was highly correlated with log centroid size (Procrustes ANOVA, $p = 0.001$, Z = 4.5, R2 = 0.23), as well as in genera *Bubalus* ($p = 0.004$, Z = 2.38, R2 = 0.23) and *Syncerus* ($p = 0.015$, Z = 2.16, R2 = 0.15), but not in *Bos* ($p = 0.075$, Z = 2.10, R2 = 0.14). The relationships of shape and size among *Bos*, *Bubalus*, and *Syncerus* were significantly different in intercept, reflecting baseline shape differences ($p = 0.001$, Z = 4.2, R2= 0.18), but not in slope (interaction of size and genus, $p = 0.11$, Z = 1.3, R2 = 0.04). Visualizing the regression score of shape on size against log centroid size (Fig. 11A) confirms similar slopes but large differences in intercept, particularly between *Syncerus* and *Bubalus* on one hand, and *Bos* (including *Bison*) on the other.

Analysis of *Ugandax* and *Syncerus*

In the analysis including just *Syncerus* spp. and *Ugandax demissum*, the first four principal components explained 31 %, 15 %, 12 % and 9 % of the variation, respectively (Fig. 12). The cranial shape changes associated with the extremes of first three principal components are shown in Figure 9B. Both the estimation of missing landmark coordinates and the removal of fossils had little effect on the principal components space (Appendices 8; 10; 12; 14).

PC1 and PC3 reflect facial elongation, cranial depth, and the flatness of the dorsal cranial surface. (PC1 negative end and PC3 positive end, Figure 9B). *Ugandax demissum*, *Sy. ekosowan* n. sp., and one specimen of *Sy. antiquus* (NHMUK PV M 34562) are close to or within the 95 % range of *Sy. caffer* along the first four principal components. The other specimen of *Sy. antiquus* (Atbara 20-88) is strongly separated from *Sy. caffer* along both PC1 and PC3.

In contrast to the relationship in Bovini, PC1 is correlated positively with log centroid size (Spearman's rank correlation test, $p < 0.05$, rho = 0.50, $R^{2} = 0.25$), indicating that facial elongation decreases with increasing size (Fig. 10B). This relationship is even stronger when only individuals of *Sy. caffer* were considered ($p < 0.01$, rho = 0.78, R2 = 0.61). Atbara 20-88, the largest cranium and that with the most negative PC1 score, is a prominent outlier to this relationship, possibly reflecting an artifact of distortion (dorsoventral compression) during fossilization. Analyses excluding fossil specimens confirm this relationship in *Sy. caffer* (Appendices 8; 10).

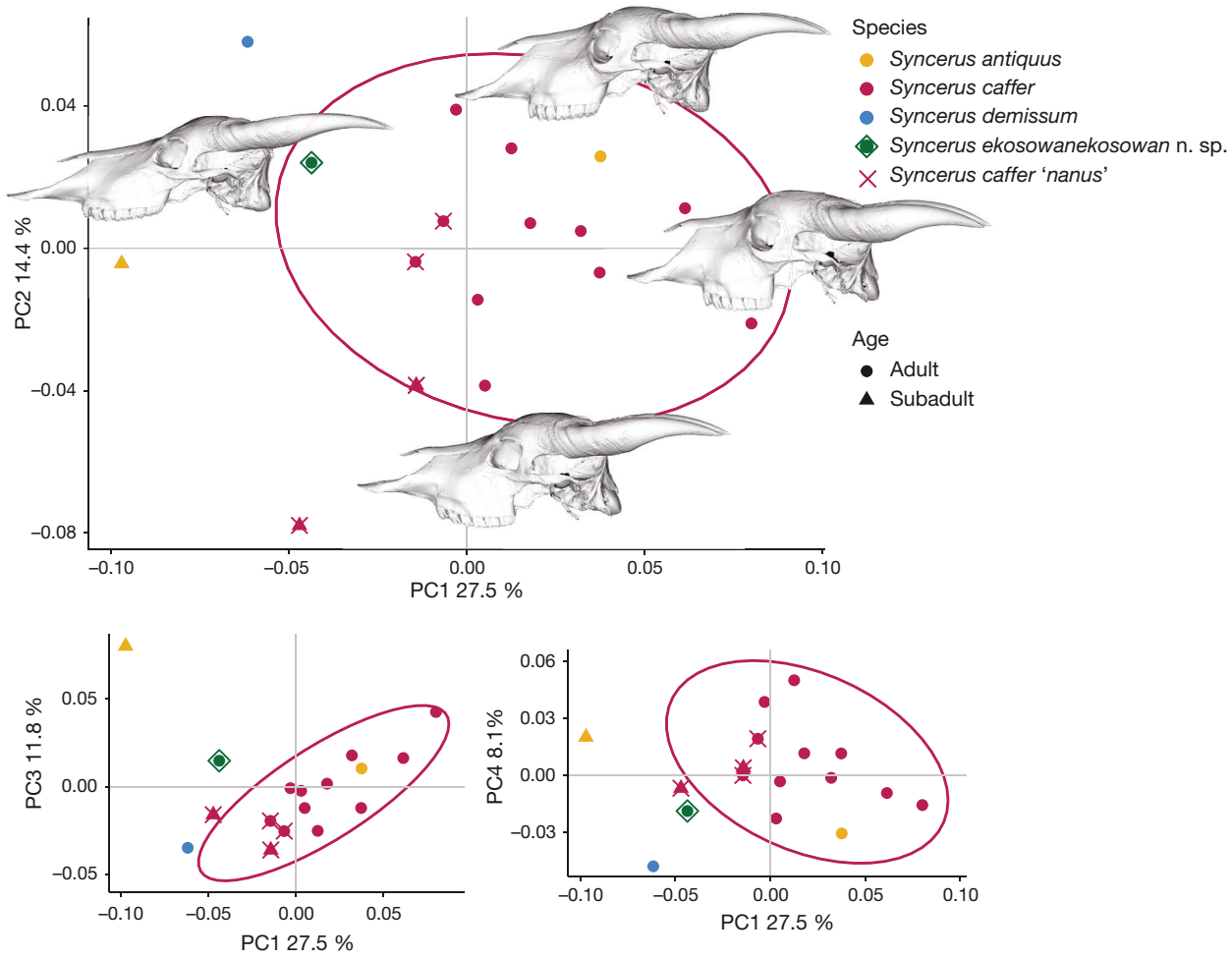

Fig. 12. — The first four principal components of cranial shape in *Syncerus* Hodgson, 1847 and *Ugandax* Cooke & Coryndon, 1970. The new cranium is similar to subadult and short-horned ('nanus') adult individuals of *Sy. caffer* (Sparrman, 1779). The position of one specimen of *Sy. antiquus* (Duvernoy, 1851) at the extremes of the first principal component (**PC1**) and **PC3** likely reflects deformation (dorsoventral compression) during fossilization. See Appendix 13 for version with specimen labels and Appendix 14 for analysis without fossil specimens.

A plot of the regression score of shape on size shows that *Syncerus ekosowan* n. sp., *Sy. antiquus*, and *U. demissum* fall close to the size-shape relationship of *Sy. caffer* (Fig. 11; Appendix 9). Even though it is an adult, OMO 53-10001 is in the size range of immature specimens of *Sy. caffer*. The fossil crania of *Sy. antiquus* are as large or larger than the largest *Sy. caffer* in our sample. At least one of these (NHMUK PV M 34563) is located within the confidence interval of the allometric regression for *Sy. caffer* (Fig. 11B). Cranial shape and log centroid size were correlated among all *Syncerus* and *Ugandax* specimens (Procrustes ANOVA, p = 0.04, Z = 1.8, R2 = 0.11) and in *Sy. caffer* alone (p = 0.001, Z = 2.9, R2 = 0.23).

DISCUSSION

The first *Syncerus*

The discovery of OMO 53-10001 C provides a basis for the naming of the oldest and most primitive species of *Syncerus*. The main diagnostic features allying the new species with *Syncerus* and distinguishing it from the more primitive *Ugandax* are the more inclined, divergent, and compressed horns with a more anteriorly located posterolateral keel, and perhaps also a reduced auditory bulla. *Syncerus ekosowan* n. sp. also displays relatively stouter horns than in *Ugandax* species (basal dimensions are similar, though cranial size is smaller). Morphological variation is high, however, and isolated horn cores or cranial fragments can be difficult to distinguish. Our findings support Gentry's (1985) initial assignment of the Shungura Formation material to *Syncerus*, and the establishment of a new species.

Conserved cranial allometry in *Syncerus*

Our results suggest that cranial diversification within *Syncerus* occurred largely along a conserved allometric trajectory. Both fossil and extant specimens – including the new Shungura cranium – lie on or close to the size–shape relationship defined by living *Sy. caffer*. (Fig. 11). The new cranium falls outside the 95 % confidence intervals but so do several specimens of *Sy. caffer* and one of two specimens of *Sy. antiquus*. Larger samples are required to know whether

these deviations represent significant biological differences, a wide range of intraspecific variation, or the effects of fossil deformation (e.g., dorsoventral compression). Nonetheless, the high similarity of all fossil specimens of *Ugandax* and *Syncerus*, including the new Shungura cranium, to the size and shape of *Sy. caffer* provides support for the hypothesis that cranial morphological disparity in this clade reflects scaling of a single underlying developmental program, rather than repeated independent innovations.*Syncerus ekosowan* n. sp. may therefore represent an ancestral "template" for the origin of later *Syncerus* forms.

The consistency of the Shungura remains suggest that its small body size and short, divergent horns are unlikely to reflect miniaturization, but rather an early stage from which larger-bodied, long-horned species later evolved. While delayed maturation of body and horn growth relative to reproductive maturity is a classic example of neoteny (reviewed in Gould 1977), the evolutionary trajectory from a small, short-horned ancestor such as *Sy. ekosowan* n. sp. to large, long-horned taxa like *Sy. acoelotus*, *Sy. antiquus*, and *Sy. caffer* is better interpreted as peramorphosis. In this case, the evidence suggests hypermorphosis – extension of the growth period – rather than acceleration of developmental rates, consistent with observations in other bovid species (Estes *et al.* 1974; Vrba 1996).

Ecomorphs and Shungura habitats

In analogy to extant *Sy. caffer* '*nanus*', Gentry (1985) suggested that the small Shungura *Syncerus* indicated the presence of woodland or forest habitats: "It looks as if the *Syncerus* lineage could long have shown a degree of morphological plasticity as an adaptive response to different environments, and one might conclude that forest or woodland environments were more widespread in the Omo area during member C time than before or after that time" (Gentry 1985: 142). However, as noted above, we do not see a large range of morphological variation as might be expected if *Sy. ekosowan* n. sp. was a highly plastic species. Unlike in *Sy. caffer*, the habitat preferences of *Sy. ekosowan* n. sp. cannot be assumed from its size and cranial form but require paleoecological analyses. Stable carbon isotope data indicate that Shungura bovins between Members C and G had C_4-dominated – i.e., most likely grass-dominated – diets (Negash *et al.* 2020). While isolated dental specimens cannot be assigned with confidence to species, *Sy. ekosowan* n. sp. is by far the most abundant bovin in the Shungura Formation based on horn core specimens and so presumably some or most of the bovin teeth analyzed by Negash *et al.* (2020) belonged to this species. Grass-eating does not, however, preclude forest or wooded habitats, as even forest buffalo today prefer grazing in clearings or along roads and rivers (Bekhuis *et al.* 2008; Prins & Sinclair 2013), though individuals from the Ituri Forest were found to have pure C_3 diets (Cerling *et al.* 2004). It has been suggested that the ancestral niche for *Sy. caffer* was in open marshy areas namely at the interface between savanna and rainforest (Bekhuis *et al.* 2008; Prins & Sinclair 2013), a plausible hypothesis also for *Syncerus ekosowan* n. sp.

Phenotypic diversification in Bovini

Our geometric morphometric analyses also provide insights into phenotypic diversification in the Bovini clade. Similar cranial shape and size-shape allometries in *Syncerus* and *Bubalus* confirm the greater similarity of African and Asian buffaloes (i.e., Bubalina) to each other than to *Bos* (Bovina). As in *Syncerus*, size-shape allometry appears to have been equally important in the phenotypic diversification of *Bubalus*, explaining much (23 %) of the cranial shape variation between mainland water buffalo (*Bu. arnee*) and island dwarfs such as the tamaraw and anoas (*Bu. mindorensis*, *Bu. depressicornis*, *Bu. quarlesi*). Further studies could investigate whether the proposed ancestors of *Bubalus*, the fossil forms *Hemibos* and *Proamphibos*, lie along the same size-shape regression. Our analysis also revealed a much greater degree of cranial disparity in *Bos* than in *Syncerus* and *Bubalus*. This is interesting considering that *Bos* diversified more recently than the buffaloes (Hassanin *et al.* 2012, 2013; Bibi 2013), implying faster rates of phenotypic evolution. The extinct *Pelorovis turkanensis* shows several aspects of cranial shape in common with species of *Bos*. (Figs 8; 10), and the proposal that it should be reassigned to this genus is worth further consideration (Martínez-Navarro *et al.* 2007). However, the claim by these same authors that it is directly ancestral to *Bos primigenius* (including *Bos taurus*) is contradicted by autapomorphic features in the skull of *Pelorovis*, the existence both past and present of diverse *Bos* lineages in Eurasia, and molecular phylogenies, which indicate a divergence of *Bos primigenius* and *Bos javanicus* during the Early or Middle Pleistocene, with a probable Asian origin (Hassanin *et al.* 2013).

Craniofacial allometry in Bovini

Species of Bovini follow the rule of cranial evolutionary allometry (CREA) (Cardini 2019), whereby larger species have relatively longer and more gracile faces (as represented by PC1, Figs 9A; 10A). Because facial gracility results in a weaker bite force relative to size, the trend to longer faces with increasing size in Bovini likely reflects consistent bite force demands (functional homogeneity) across the allometric gradient (Zelditch & Swiderski 2023; Mitchell *et al.* 2024). This might be expected in grazers, given that grasses are more homogeneously nutritious and overall less fibrous and lignified than browse (Jarman 1974). The correlation of size and facial elongation is, however, not significant within genera (*Bos*, *Bubalus*, *Syncerus*, Fig. 10A). Interestingly, when *Syncerus* and *Ugandax* were analyzed separately, the relationship was inverted, with facial shortening accompanying increasing size (Fig. 10B). The presence of a fossil specimen as an extreme outlier along PC1 (*Sy. antiquus* Atbara 20-88) made interpretation of the relationship across *Syncerus*, however, unclear (Fig. 10B). Examining the ontogenetic allometry in *Sy. caffer* confirmed the correlation of larger size with shorter faces in this species (Fig. 10B; Appendix 10B). Inverted growth and evolutionary allometries were also noted in several rodent lineages, and likely reflect growth constraints, namely the fact that infants are born without fully formed teeth and jaw muscles, and increase in facial robusticity with age (Zelditch & Swiderski 2023).

While inverse craniofacial allometry might represent selection for greater bite force requirements with increasing size (Mitchell *et al.* 2024), there seems to be no evidence for dietary differences between young and adults of *Sy. caffer* (Prins & Sinclair 2013). Whether an inverse CREA rule characterizes the evolutionary allometry of *Syncerus* as whole should be established with further work using larger fossil sample sizes.

Departures from shared allometry

A large proportion of cranial shape variation is, however, not determined by size, leaving room for species-specific innovations, particularly in horn morphology. While our examination of horn core length relative to basal size in bovins showed that the new Shungura species shares the relatively shorter horns of other *Syncerus* species, they revealed that another species departs significantly from the length-size allometry of *Syncerus*. Horn cores of the giant buffalo *Sy. antiquus* can reach over 1.5 m in length, far greater than predicted by allometry in the *Syncerus* clade (Fig. 6B). This contrasts with the large antlers of the giant elk, which, as Gould (1974) famously demonstrated, can be predicted by the general allometric relationship of body size and antler length in deer. Strong selective pressures might have been behind the evolution of the great horn span of the giant buffalo, resulting in a significant departure away from the conserved length to size relationship in the *Syncerus* clade. This supports the proposal that secondary sexual characters such as horns and other weapons or ornaments can evolve rapidly, especially following population isolation (West-Eberhard 1983; Vrba 1995; Emlen 2008).

The extreme horn length of *Sy. antiquus* likely reflects prolonged post-maturational growth of horn cores, analogous to patterns seen in extant buffalo, sheep (*Ovis* Linnaeus, 1758), and in other continuously growing structures such as elephant tusks (*Loxodonta* Anonymous, 1827, *Elephas* Linnaeus, 1758) and giraffe ossicones (*Giraffa* Brisson, 1762), with such extension of growth duration in secondary sexual characters typically associated with territoriality and living in large groups (Estes *et al.* 1974). However, while living bovins are gregarious, they are all non-territorial, and it is reasonable to infer that the giant buffalo shared this social system. The selective context for such extreme weaponry therefore remains uncertain, but any interpretation would also have to explain other extreme examples such as the long-horned bison (*Bison latifrons*), where escalation in size and weaponry also likely represents lineage-specific departures from otherwise conserved allometry.

CONCLUSIONS

The new material of *Syncerus* material from the Shungura Formation provides the earliest well-preserved evidence of the African buffalo genus. These fossils, including a nearly complete cranium, document a small-bodied, short-horned species, *Sy. ekosowan* n. sp., that predates the better-known Pleistocene representatives of the genus. Geometric morphometric analyses suggest that *Sy. ekosowan* n. sp. and other early *Syncerus* specimens follow the same cranial allometric trajectory as extant *Sy. caffer*, tentatively supporting the view that much of the morphological diversification within the clade arose through conserved growth patterns. This conserved trajectory helps to explain the striking eco-morphological variation among modern African buffalo, in which forest and savanna morphotypes can be understood as heterochronic outcomes along a shared developmental pathway. At the same time, the extreme horn length of *Sy. antiquus* represents a clear departure from this pattern, highlighting the potential for lineage-specific innovations in secondary sexual traits.

More broadly, these findings underscore both the value of new fossil discoveries and the need for larger comparative samples. Expanding the fossil record and integrating it with developmental analyses will be essential for describing the full range of cranial and horn diversity in *Syncerus*, and for uncovering the developmental mechanisms by which evolutionary constraint and innovation combined to shape the clade. Equally important is further investigation of ecophenotypic plasticity in extant *Sy. caffer*, and the search for traces of such plasticity in the fossil record. This will require not only new and larger fossil samples, but also a critical revision of existing museum collections.

Acknowledgements

This study was supported by German Research Foundation (Deutsche Forschungsgemeinschaft, DFG) project number 282995372 to F.B. and conducted within the framework of the Omo Group Research Expedition (OGRE) field and lab work. The OGRE is a joint program of PALEVOPRIM, the CFEE and the EHA principally funded by the Ministry of Europe and Foreign Affairs, the National Research Agency, the Région Nouvelle-Aquitaine, CNRS INEE, PALEVOPRIM, and the Fyssen Foundation. The OGRE is extremely grateful to the Ethiopian Heritage Authority, the SNNPR, the South Omo Zone, the Nyangatom and Dassanetch Weredas and their people for their help and reception. The specimen from the Middle Atbara, Sudan, was collected as part of fieldwork funded by the German Research Foundation (DFG project 387794796 to F.B.), and that from Singa studied with the support of the European Research Council (ERC Consolidator Grant, PALEONILE, project 101045217). We are indebted to the hundreds of people who participated in the fieldwork missions of the IORE, OGRE, and other research projects, who managed collections and databases, prepared specimens, contributed to their study, provided financial support, helped with administrative processes, and provided advice and moral support. We thank the National Museum of Ethiopia/Ethiopian Heritage Authority (formerly ARCCH, Ministry of Tourism) for allowing access to the collections and research, NME/EHA staff for support with collection study, Tim White and the Middle Awash Project for access to specimens, and A. Gigliotti, L. Janzen, K. Mahlow, P. Mahlow, L. Rose, K. Salih, and J. Tyler for assistance with 3D scanning. This article has undergone a dual peer-review, initially by *PCI*

Paleontology (recommendation https://doi.org/10.24072/pci.paleo.100399), and subsequently by the *Comptes Rendus Palevol*. We thank V. Weisbecker (*PCI* recommender), R. Mitchell, and a second anonymous reviewer for comments that significantly improved this manuscript.

Data, script, and code availability

Raw data files and R scripts for reproducing all analyses are available at: https://doi.org/10.17605/OSF.IO/WCAVJ

Author contributions

J.-R.B led field research and new specimen acquisition; F.B. designed the study; J.-R.B. curated specimen data; F.B. performed the analyses and interpreted the results; F.B. and J.-R.B. acquired funding; F.B. wrote the manuscript with comments and revisions from J.-R.B.

REFERENCES

Abbate E., Albianelli A., Awad A., Billi P., Bruni P., Delfino M., Ferretti M. P., Filippi O., Gallai G., Ghinassi M., Lauritzen S.-E., Vetro D. L., Martínez-Navarro B., Martini F., Napoleone G., Bedri O., Papini M., Rook L. & Sagri M. 2010. — Pleistocene environments and human presence in the middle Atbara valley (Khashm El Girba, Eastern Sudan). *Palaeogeography, Palaeoclimatology, Palaeoecology* 292 (1-2): 12-34. https://doi.org/10.1016/j.palaeo.2010.03.022

Adams D. C., Collyer M. L., Kaliontzopoulou A. & Baken E. K. 2023. — *Geomorph: Software for geometric morphometric analyses*. R package version 4.0.6.

Arambourg C. 1947. — *Contribution a l'étude géologique et paléontologique du bassin du Lac Rodolphe et de la basse vallée de l'Omo. Mission Scientifique de l'Omo, 1932-1933. Géologie-Anthropologie*. Vol. 3. Muséum national d'Histoire naturelle, Paris: 75-406.

Arambourg C., Chavaillon J. & Coppens Y. 1967. — Premiers résultats de la nouvelle mission de l'Omo (1967). *Comptes Rendus des Séances de l'Académie des Sciences, Paris* 265: 1891-1896.

Baird C. N., Ernst M., Waurick I., Blom M. P. K. & Bibi F. 2023. — Integrative taxonomy using historical specimens provides evidence for a single species of bushbuck, *Tragelaphus scriptus* (Mammalia: Bovidae). *Zoological Journal of the Linnean Society* 200 (2): 532-546. https://doi.org/10.1093/zoolinnean/zlad096

Baken E. K., Collyer M. L., Kaliontzopoulou A. & Adams D. C. 2021. — geomorph v4.0 and gmShiny: enhanced analytics and a new graphical interface for a comprehensive morphometric experience. *Methods in Ecology and Evolution* 12 (12): 2355-2363. https://doi.org/10.1111/2041-210X.13723

Bate D. M. 1951. — The mammals from Singa and Abu Hugar. *Fossil Mammals of Africa* 2: 1-28.

Bekhuis P. D. B. M., De Jong C. B. & Prins H. H. T. 2008 — Diet selection and density estimates of forest buffalo in Campo-Ma'an National Park, Cameroon. *African Journal of Ecology* 46 (4): 668-675. https://doi.org/10.1111/j.1365-2028.2008.00956.x

Bhullar B.-A. S., Marugán-Lobón J., Racimo F., Bever G. S., Rowe T. B., Norell M. A. & Abzhanov A. 2012. — Birds have paedomorphic dinosaur skulls. *Nature* 487 (7406): 223-226. https://doi.org/10.1038/nature11146

Bibi F. 2009. — *Evolution, systematics, and paleoecology of Bovinae (Mammalia: Artiodactyla) from the late Miocene to the Recent.* PhD Dissertation, Yale University, New Haven, Connecticut, 469 p.

Bibi F. 2023. — The mammal dental metrics database: a compilation of fossil and extant mammal tooth measurements. *Dryad*. https://doi.org/10.5061/dryad.69p8cz968

Bibi F. 2013. — A multi-calibrated mitochondrial phylogeny of extant Bovidae (Artiodactyla, Ruminantia) and the importance of the fossil record to systematics. *BMC Evolutionary Biology* 13 (1): 166. https://doi.org/10.1186/1471-2148-13-166

Bibi F. & Boisserie J.-R. 2025. — Supplementary data accompanying article: a new fossil buffalo from the Shungura Formation (Ethiopia) reveals the role of heterochrony in the evolution of *Syncerus*. https://doi.org/10.17605/OSF.IO/WCAVJ

Bibi F., Rowan J. & Reed K. 2017. — Late Pliocene Bovidae from Ledi-Geraru (Lower Awash Valley, Ethiopia) and their implications for Afar paleoecology. *Journal of Vertebrate Paleontology* 37 (4): e1337639. https://doi.org/10.1080/02724634.2017.1337639

Bibi F. & Tyler J. 2022. — Evolution of the bovid cranium: morphological diversification under allometric constraint. *Communications Biology* 5 (1): 1-12. https://doi.org/10.1038/s42003-021-02877-6

Bibi F. & Tyler J. 2021. — Evolution of the bovid cranium: Morphological diversification under allometric constraint [Dataset]. https://doi.org/10.7479/499J-TV94

Boisserie J.-R., Guy F., Delagnes A., Hlukso L. J., Bibi F., Beyene Y. & Guillemot C. 2008. — New palaeoanthropological research in the Plio-Pleistocene Omo Group, Lower Omo Valley, SNNPR (Southern Nations, Nationalities and People Regions), Ethiopia. *Comptes Rendus Palevol* 7 (7): 429-439. https://doi.org/10.1016/j.crpv.2008.07.010

Cardini A. 2019. — Craniofacial allometry is a rule in evolutionary radiations of placentals. *Evolutionary Biology* 46 (3): 239-248. https://doi.org/10.1007/s11692-019-09477-7

Cerling T. E., Hart J. A. & Hart T. B. 2004. — Stable isotope ecology in the Ituri Forest. *Oecologia* 138 (1): 5-12. https://doi.org/10.1007/s00442-003-1375-4

Churcher C. S. 1972. — *Late Pleistocene vertebrates from archaeological sites in the Plain of Kom Ombo, Upper Egypt*. Royal Ontario Museum, Toronto, 172 p. https://doi.org/10.5962/bhl.title.52073

Codron D., Hofmann R. R. & Clauss M. 2019. — Morphological and physiological adaptations for browsing and grazing, *in* Gordon I. J. & Prins H. H. T. (eds), *The Ecology of Browsing and Grazing II. Ecological Studies* Vol. 239. Springer International Publishing, Cham: 81-125. https://doi.org/10.1007/978-3-030-25865-8_4

Collyer M. L. & Adams D. C. 2021. — RRPP: Linear Model Evaluation with Randomized Residuals in a Permutation Procedure, R package version 1.4.0.

Collyer M. L. & Adams D. C. 2018. — RRPP: An R package for fitting linear models to high-dimensional data using residual randomization. *Methods in Ecology and Evolution* 9 (7): 1772-1779. https://doi.org/10.1111/2041-210X.13029

Cooke H. B. S. & Coryndon S. C. 1970. — Pleistocene mammals from the Kaiso Formation and other related deposits in Uganda, *in* Leakey L. S. B. & Savage R. J. G. (eds), *Fossil Vertebrates of Africa*. Vol. 2. Academic Press, London: 107-224.

Damuth J. & Janis C. M. 2011. — On the relationship between hypsodonty and feeding ecology in ungulate mammals, and its utility in palaeoecology. *Biological Reviews* 86 (3): 733-758. https://doi.org/10.1111/j.1469-185X.2011.00176.x

De Heinzelin J. 1983. — *The Omo Group: Archives of the International Omo Research Expedition*. Musée Royal de l'Afrique Centrale, Teruvren, 365 p.

Drake A. G. & Klingenberg C. P. 2008. — The pace of morphological change: historical transformation of skull shape in St Bernard dogs. *Proceedings of the Royal Society B: Biological Sciences* 275 (1630): 71-76. https://doi.org/10.1098/rspb.2007.1169

Emlen D. J. 2008. — The evolution of animal weapons. *Annual Review of Ecology, Evolution, and Systematics* 39 (1): 387-413. https://doi.org/10.1146/annurev.ecolsys.39.110707.173502

ESTES R. D., GEIST V. & WALTHER F. 1974. — Social organization of the African Bovidae, *in* GEIST V. & WALTHER F. R. (eds), *The Behaviour of Ungulates and its Relation to Management*. IUCNNR, Morges: 166-205.

EVERETT M. A. 2010. — *The paleoecology of the Pleistocene Upper Busidima Formation, Gona, Afar Depression, Ethiopia*. Indiana University, Bloomington, Indiana, 423 p.

FAITH J. T., ROWAN J. & DU A. 2019. — Early hominins evolved within non-analog ecosystems. *Proceedings of the National Academy of Sciences* 116 (43): 21478-21483. https://doi.org/10.1073/pnas.1909284116

FAITH J. T., ROWAN J., O'BRIEN K., BLEGEN N. & PEPPE D. J. 2020. — Late Pleistocene mammals from Kibogo, Kenya: systematic paleontology, paleoenvironments, and non-analog associations. *Journal of Vertebrate Paleontology* 40 (5): e1841781. https://doi.org/10.1080/02724634.2020.1841781

FAITH J. T., TRYON C. A., PEPPE D. J., BEVERLY E. J., BLEGEN N., BLUMENTHAL S., CHRITZ K. L., DRIESE S. G. & PATTERSON D. 2015. — Paleoenvironmental context of the Middle Stone Age record from Karungu, Lake Victoria Basin, Kenya, and its implications for human and faunal dispersals in East Africa. *Journal of Human Evolution* 83: 28-45. https://doi.org/10.1016/j.jhevol.2015.03.004

FARKE A. A. 2010. — Evolution and functional morphology of the frontal sinuses in Bovidae (Mammalia: Artiodactyla), and implications for the evolution of cranial pneumaticity. *Zoological Journal of the Linnean Society* 159 (4): 988-1014. https://doi.org/10.1111/j.1096-3642.2009.00586.x

GARDIN A., PUCÉAT E., GARCIA G., BOISSERIE J.-R., EURIAT A., JOACHIMSKI M. M., NUTZ A., SCHUSTER M. & OTERO O. 2024. — Stable oxygen isotopes of crocodilian tooth enamel allow tracking Plio-Pleistocene evolution of freshwater environments and climate in the Shungura Formation (Turkana Depression, Ethiopia). *Biogeosciences* 21 (2): 437-454. https://doi.org/10.5194/bg-21-437-2024

GAUTIER A. & MUZZOLINI A. HO 1991. — The life and times of the Giant Buffalo alias *Bubalus*/*Homoioceras*/*Pelorovis antiquus* in North Africa. *Archaeozoologia* 4 (1): 39-92.

GEIST V. 1971. — *Mountain sheep: A study in behavior and evolution*. University of Chicago Press, Chicago, 384 p.

GENTRY A. W. 2011. — Bovidae, *in* HARRISON T. (ed.), *Paleontology and Geology of Laetoli: Human Evolution in Context*. Vol. 2. Springer, New York: 363-465.

GENTRY A. W. 2010. — Bovidae, *in* WERDELIN L. & SANDERS W. J. (eds), *Cenozoic Mammals of Africa*. University of California Press, Berkeley: 747-803.

GENTRY A. W. 2006. — A new bovine (Bovidae, Artiodactyla) from the Hadar Formation, Ethiopia. *Transactions of the Royal Society of South Africa* 61 (2): 41-50. https://doi.org/10.1080/00359190609519952

GENTRY A. W. 1990. — The Semliki fossil bovids, *in* BOAZ N. T. (ed.), *Evolution of Environments and Hominidae in the African Western Rift Valley*. Virginia Museum of Natural History, Martinsville: 225-234. (Virginia Museum of Natural History Memoir).

GENTRY A. W. 1987. — Pliocene Bovidae from Laetoli, *in* LEAKEY M. D. & HARRIS J. M. (eds), *Laetoli: A Pliocene Site in Northern Tanzania*. Clarendon Press, Oxford: 378-408.

GENTRY A. W. 1985. — The Bovidae of the Omo Group deposits, Ethiopia (French and American collections), *in* COPPENS Y. & HOWELL F. C. (eds), *Les faunes Plio-Pléistocènes de la basse Vallée de l'Omo (Ethiopie); I: Perissodactyles-Artiodactyles (Bovidae)*. CNRS, Paris: 119-191. (Cahiers de Paléontologie.).

GENTRY A. W. 1980. — Fossil Bovidae (Mammalia) from Langebaanweg, South Africa. *Annals of the South African Museum* 79 (8): 213-337. https://www.biodiversitylibrary.org/part/74624

GENTRY A. W. 1967. — *Pelorovis oldowayensis* Reck, an extinct bovid from East Africa. *Bulletin of the British Museum (Natural History) Geology Series* 14 (7): 245-299. https://www.biodiversitylibrary.org/part/83479

GENTRY A. W. & GENTRY A. 1978. — Fossil Bovidae (Mammalia) of Olduvai Gorge, Tanzania; Part I. *Bulletin of the British Museum. Natural History. Geology Series* 29 (4): 289-446. https://www.biodiversitylibrary.org/part/83406

GERAADS D. 1995. — *Simatherium shungurense* n. sp., un noveau Bovini (Artiodactyla, Mammalia) du Pliocène terminal de l'Omo (Éthiopie). *Annales de Paléontologie* 81: 87-96.

GERAADS D. & THOMAS H. 1994. — Bovidés du Plio-Pléistocène d'Ouganda, *in* SENUT B. & PICKFORD M. (eds), *Geology and Palaeobiology of the Albertine Rift Valley, Uganda-Zaire; Volume II, Palaeobiology*.Vol. 29. CIFEG, Paris: 383-407.

GERAADS D., BOBE R. & REED K. 2012. — Pliocene Bovidae (Mammalia) from the Hadar Formation of Hadar and Ledi-Geraru, Lower Awash, Ethiopia. *Journal of Vertebrate Paleontology* 32 (1): 180-197. https://doi.org/10.1080/02724634.2012.632046

GILBERT W. H. 2008. — Bovidae, *in* GILBERT W. H. & ASFAW B. (eds), Homo erectus*: Pleistocene Evidence from the Middle Awash, Ethiopia*. University of California Press, Berkeley: 45-94.

GOMES RODRIGUES H., CORNETTE R., CLAVEL J., CASSINI G., BHULLAR B.-A. S., FERNÁNDEZ-MONESCILLO M., MORENO K., HERREL A. & BILLET G. 2018. — Differential influences of allometry, phylogeny and environment on the rostral shape diversity of extinct South American notoungulates. *Royal Society Open Science* 5 (1): 171816. https://doi.org/10.1098/rsos.171816

GOULD S. J. 1977. — *Ontogeny and Phylogeny*. Cambridge, Mass. London, England, Belknap Press of Havard University Press. 501 p.

GOULD S. J. 1974. — The origin and function of 'bizzare' structures: Antler size and skull size in the 'Irish elk', *Megaloceros giganteus*. *Evolution* 28 (2): 191-220. https://doi.org/10.1111/j.1558-5646.1974.tb00740.x

GRUBB P. 1972. — Variation and incipient speciation in the African buffalo. *Zeitschrift für Säugetierkunde* 37: 121-144. https://www.biodiversitylibrary.org/part/191230

GRUBB P. 2005. — Family Bovidae, *in* WILSON D. E. & REEDER D. A. M. (eds), *Mammals Species of the World: A Taxonomic and Geographic Reference*. Vol. 1. Johns Hopkins University Press, Baltimore: 673-722.

HAILE-SELASSIE Y., VRBA E. S. & BIBI F. 2009. — Bovidae, *in* HAILE-SELASSIE Y. & WOLDEGABRIEL G. (eds), Ardipithecus kadabba*: Late Miocene Evidence from the Middle Awash, Ethiopia*. University of California Press, Berkeley: 277-330.

HARRIS J. M. 2003. — Bovidae from the Lothagam succession, *in* LEAKEY M. G. & HARRIS J. M. (eds), *Lothagam: The Dawn of Humanity in Eastern Africa*. Columbia University Press, New York: 531-579.

HARRIS J. M. 1991. — Family Bovidae, *in* HARRIS J. M. (ed.), *Koobi Fora Research Project Volume 3: The Fossil Ungulates: Geology, Fossil Artiodactyls, and Palaeoenvironments.* Clarendon Press, Oxford: 139-320.

HARRIS J. M., BROWN F. H. & LEAKEY M. G. 1988. — Stratigraphy and paleontology of Pliocene and Pleistocene localities west of Lake Turkana, Kenya. *Contributions in Science* 399: 1-128. https://doi.org/10.5962/p.241284

HARRIS J. M., LEAKEY M. G., CERLING C. E. & WINKLER A. J. 2003. — Early Pliocene tetrapod remains from Kanapoi, Lake Turkana Basin, Kenya. *Contributions in Science* 498: 39-114. https://doi.org/10.5962/p.226790

HASSANIN A., AN J., ROPIQUET A., NGUYEN T. T. & COULOUX A. 2013. — Combining multiple autosomal introns for studying shallow phylogeny and taxonomy of Laurasiatherian mammals: Application to the tribe Bovini (Cetartiodactyla, Bovidae). *Molecular Phylogenetics and Evolution* 66 (3): 766-775. https://doi.org/10.1016/j.ympev.2012.11.003

HASSANIN A., DELSUC F., ROPIQUET A., HAMMER C., JANSEN VAN VUUREN B., MATTHEE C., RUIZ-GARCIA M., CATZEFLIS F., ARESKOUG V., NGUYEN T. T. & COULOUX A. 2012. — Pattern

and timing of diversification of Cetartiodactyla (Mammalia, Laurasiatheria), as revealed by a comprehensive analysis of mitochondrial genomes. *Comptes Rendus Biologies* 335 (1): 32-50. https://doi.org/10.1016/j.crvi.2011.11.002

HODGSON B. H. 1847. — On the mammals of Nepal. *Journal of the Asiatic Society of Bengal* 16: 685-711.

HOWELL F. C. 1968. — Omo Research Expedition. *Nature* 219 (5154): 567-572. https://doi.org/10.1038/219567a0

HUXLEY J. 1932. — *Problems of Relative Growth*. The Dial Press, New York, 276 p.

JANIS C. M. 1990. — Correlation of cranial and dental variables with body size in ungulates and macropodoids, *in* DAMUTH J. & MACFADDEN B. J. (eds), *Body Size in Mammalian Paleobiology*. Cambridge University Press, Cambridge: 255-300.

JARMAN P. J. 1974. — The social organisation of antelope in relation to their ecology. *Behaviour* 48 (1-4): 215-267. https://doi.org/10.1163/156853974X00345

KAMMERER C. F., DEUTSCH M., LUNGMUS J. K. & ANGIELCZYK K. D. 2020. — Effects of taphonomic deformation on geometric morphometric analysis of fossils: a study using the dicynodont *Diictodon feliceps* (Therapsida, Anomodontia). *PeerJ* 8: e9925. https://doi.org/10.7717/peerj.9925

KIDANE T., BROWN F. H. & KIDNEY C. 2014. — Magnetostratigraphy of the Fossil-Rich Shungura Formation, southwest Ethiopia. *Journal of African Earth Sciences* 97: 207-223. https://doi.org/10.1016/j.jafrearsci.2014.05.005

KLEIN R. G. 1994. — The long-horned African buffal (*Pelorovis antiquus*) is an extinct species. *Journal of Archaeological Science* 21 (6): 725-733. https://doi.org/10.1006/jasc.1994.1072

KLINGENBERG C. P. 2016. — Size, shape, and form: concepts of allometry in geometric morphometrics. *Development Genes and Evolution* 226 (3): 113-137. https://doi.org/10.1007/s00427-016-0539-2

KRONE I. W., KAMMERER C. F. & ANGIELCZYK K. D. 2019. — The many faces of synapsid cranial allometry. *Paleobiology* 45 (4): 531-545. https://doi.org/10.1017/pab.2019.26

LÖNNBERG T. 1933. — Description of a fossil buffalo from East Africa. *Arkiv för Zoology A* 25: 1-32.

LYDEKKER R. 1913. — *Catalogue of the Ungulate Mammals in the British Museum (Natural History).* Vol. 1. British Museum, London, 249 p.

MARTÍNEZ-NAVARRO B., ANTONIO PÉREZ-CLAROS J., PALOMBO M. R., ROOK L. & PALMQVIST P. 2007. — The Olduvai buffalo *Pelorovis* and the origin of *Bos*. *Quaternary Research* 68 (2): 220-226. https://doi.org/10.1016/j.yqres.2007.06.002

MCDOUGALL I. & BROWN F. H. 2008. — Geochronology of the pre-KBS Tuff sequence, Omo Group, Turkana Basin. *Journal of the Geological Society* 165 (2): 549-562. https://doi.org/10.1144/0016-76492006-170

MCDOUGALL I. & BROWN F. H. 2006. — Precise ^{40}Ar/ ^{39}Ar geochronology for the upper Koobi Fora Formation, Turkana Basin, northern Kenya. *Journal of the Geological Society* 163 (1): 205-220. https://doi.org/10.1144/0016-764904-166

MCDOUGALL I., BROWN F. H., VASCONCELOS P. M., COHEN B. E., THIEDE D. S. & BUCHANAN M. J. 2012. — New single crystal ^{40}Ar/^{39}Ar ages improve time scale for deposition of the Omo Group, Omo–Turkana Basin, East Africa. *Journal of the Geological Society* 169 (2): 213-226. https://doi.org/10.1144/0016-76492010-188

MITCHELL D. R., SHERRATT E. & WEISBECKER V. 2024. — Facing the facts: adaptive trade-offs along body size ranges determine mammalian craniofacial scaling. *Biological Reviews* 99 (2): 496-524. https://doi.org/10.1111/brv.13032

NEGASH E. W., ALEMSEGED Z., BOBE R., GRINE F., SPONHEIMER M. & WYNN J. G. 2020. — Dietary trends in herbivores from the Shungura Formation, southwestern Ethiopia. *Proceedings of the National Academy of Sciences* 117 (36): 21921-21927. https://doi.org/10.1073/pnas.2006982117

POMEL A. 1893. — Bubalus antiquus. Imprimerie P. Fontana, Algieria, 94 p., 10 plates.

POSIT TEAM 2025. — *RStudio: Integrated Development Environment for R*. Boston, MA, Posit Software, PBC.

PRINS H. H. T. & SINCLAIR A. R. E. 2013. — *Syncerus caffer* African Buffalo, *in* KINGDON J. & HOFFMANN M. (eds), *Mammals of Africa Vol. 6: Hippopotamuses, Pigs, Deer, Giraffe, and Bovids*. Bloomsbury, New York: 125-136.

R CORE TEAM 2025. — R: A language and environment for statistical computing.

RENNE P. R., WOLDEGABRIEL G., HART W. K., HEIKEN G. & WHITE T. D. 1999. — Chronostratigraphy of the Miocene-Pliocene Sagantole Formation, Middle Awash Valley, Afar rift, Ethiopia. *Geological Society of America Bulletin* 111 (6): 869-885. https://doi.org/10.1130/0016-7606(1999)111%3C0869:COTMPS%3E2.3.CO;2

ROWAN J., FAITH J. T., GEBRU Y. & FLEAGLE J. G. 2015. — Taxonomy and paleoecology of fossil Bovidae (Mammalia, Artiodactyla) from the Kibish Formation, southern Ethiopia: Implications for dietary change, biogeography, and the structure of the living bovid faunas of East Africa. *Palaeogeography, Palaeoclimatology, Palaeoecology* 420: 210-222. https://doi.org/10.1016/j.palaeo.2014.12.017

ROWAN J., LAZAGABASTER I. A., CAMPISANO C. J., BIBI F., BOBE R., BOISSERIE J.-R., FROST S. R., GETACHEW T., GILBERT C. C., LEWIS M. E., MELAKU S., SCOTT E., SOURON A., WERDELIN L., KIMBEL W. H. & REED K. E. 2022. — Early Pleistocene large mammals from Maka'amitalu, Hadar, lower Awash Valley, Ethiopia. *PeerJ* 10: e13210. https://doi.org/10.7717/peerj.13210

SIMONS E. A. & FROST S. R. 2021. — Ontogenetic allometry and scaling in catarrhine crania. *Journal of Anatomy* 238 (3): 693-710. https://doi.org/10.1111/joa.13331

SINCLAIR A. R. E. 1977. — *The African Buffalo*. University of Chicago Press, Chicago, 355 p.

SMITZ N., BERTHOULY C., CORNÉLIS D., HELLER R., VAN HOOFT P., CHARDONNET P., CARON A., PRINS H., VAN VUUREN B. J., DE IONGH H. & MICHAUX J. 2013. — Pan-African Genetic Structure in the African Buffalo (Syncerus caffer): Investigating Intraspecific Divergence, *in* HOFREITER M. (ed.). *PLoS ONE* 8 (2): e56235. https://doi.org/10.1371/journal.pone.0056235

SUWA G., BEYENE Y., NAKAYA H., BERNOR R. L., BOISSERIE J.-R., BIBI F., AMBROSE S. H., SANO K., KATOH S. & ASFAW B. 2015. — Newly discovered cercopithecid, equid and other mammalian fossils from the Chorora Formation, Ethiopia. *Anthropological Science* 123 (1): 19-39. https://doi.org/10.1537/ase.150206

TEJERO-CICUÉNDEZ H., MENÉNDEZ I., TALAVERA A., MOCHALES-RIAÑO G., BURRIEL-CARRANZA B., SIMÓ-RIUDALBAS M., CARRANZA S. & ADAMS D. C. 2023. — Evolution along allometric lines of least resistance: morphological differentiation in Pristurus geckos. *Evolution* 77 (12): 2547-2560. https://doi.org/10.1093/evolut/qpad166

TSUKAMOTO S., BUSSERT R., DELAGNES A., RICHTER M., MOHAMMEDNOOR M., BEDRI O., KRAATZ B., MÜLLER J., SALIH K., EISAWI A. & BIBI F. 2022. — Luminescence chronology of fossiliferous fluvial sediments along the middle Atbara River, Sudan. *Quaternary Geochronology* 71: 101312. https://doi.org/10.1016/j.quageo.2022.101312

VRBA E. S. 2004. — Ecology, evolution, and development: perspectives from the fossil record, *in* HALL B. K., PEARSON R. D. & MULLER G. B. (eds), *Environment, Development, and Evolution*. MIT Press, Cambridge, Mass.: 85-105.

VRBA E. S. 1995. — Species as habitat-specific complex systems, *in* LAMBERT D. M & SPENCER H. G (eds), *Speciation and the Recognition Concept*. Johns Hopkins University Press, Baltimore: 3-44.

VRBA E. S. 1976. — *The fossil Bovidae of Sterkfontein, Swartkrans, and Kromdraai*. Transvaal Museum, Pretoria, 166 p. (Memoir - Transvaal Museum; no. 21).

VRBA E. S., VAISNYS J. R., GATESY J. E., DESALLE R. & WEI K. Y. 1994. — Analysis of pedomorphosis using allometric characters – the example of Reduncini antelopes (Bovidae, Mammalia). *Systematic Biology* 43 (1): 92-116. https://doi.org/10.1093/sysbio/43.1.92

VRBA E. S. 1996. — Climate, heterochrony, and human evolution. *Journal of Anthropological Research* 52 (1): 1-28. https://doi.org/10.1086/jar.52.1.3630234

WEST-EBERHARD M. J. 1983. — Sexual selection, social competition, and speciation. *The Quarterly Review of Biology* 58 (2): 155-183. https://doi.org/10.1086/413215

ZELDITCH M. L. & SWIDERSKI D. L. 2023. — The Predictable complexity of evolutionary allometry. *Evolutionary Biology* 50 (1): 56-77. https://doi.org/10.1007/s11692-022-09581-1

Submitted on 19 November 2025;
accepted on 9 March 2026;
published on 29 September 2026.

APPENDICES

APPENDIX 1. — Number of landmarks missing (out of a total of 53) by specimen.

Specimen	Landmarks missing
Ugandax demissum (Gentry, 1980) GAW-VP 3 slash 210.pts	21
Simatherium shungurense Geraads, 1995 OMO 75 S-69-2733 PLY.pts	19
Bubalus arnee (Kerr, 1792) ZMB Mam 14801.pts	15
Syncerus antiquus (Duvernoy, 1851) 20-88 Buffalo skull sm.pts	15
Bos primigenius Bojanus, 1827 ZMB MB Ma 226.pts	10
Syncerus Hodgson, 1847 Fossil OMO 53 10001.pts	10
Syncerus caffer (Sparrman, 1779) YPM 16009.pts	9
Syncerus caffer YPM 3612.pts	8
Syncerus antiquus NHM_PV_M_34562_r.pts	6
Bison bison (Linnaeus, 1758) YPM 3406.pts	4
Bos primigenius MB Ma 671.pts	3
Bubalus mindorensis Heude, 1888 AMNH 99339.pts	3
Bos javanicus d'Alton, 1823 AMNH 113755.pts	2
Bos primigenius NHMUK ARC 1972 5062.pts	2
Pelorovis turkanensis Harris, 1991 KNM ER 524 (ER 70 FS 325) PLY.pts	2
Syncerus caffer ZMB Mam 108931 A104 13.pts	2
Bison bison IMNH R-163.pts	1
Bos primigenius NHMUK ARC 1972 5068.pts	1
Syncerus caffer ZMB Mam 35750.pts	1
Bison Bison YPM 3405.pts	0
Bison latifrons (Harlan, 1825) IMNH-48001_1770.pts	0
Bos gaurus C.H.Smith, 1827 ZMB 85047.pts	0
Bos gaurus ZMB Mam 14802.pts	0
Bos primigenius NHMUK ARC 1977 5012.pts	0
Bos primigenius NHMUK PV OR 50086.pts	0
Bos taurus Linnaeus, 1758 domestic NHMUK 1981_984.pts	0
Bubalus arnee (Kerr, 1792) ZMB 48424.pts	0
Bubalus depressicornis (C.H.Smith, 1827) AMNH 152856.pts	0
Bubalus depressicornis AMNH 61146.pts	0
Bubalus depressicornis ZMB 73488.pts	0
Bubalus mindorensis Heude, 1888 AMNH 40046.pts	0
Bubalus mindorensis ZMB 73510.pts	0
Bubalus quarlesi celebes ZMB 73496.pts	0
Bubalus quarlesi (Ouwens, 1910) ZMB 73484.pts	0
Syncerus caffer ZMB Mam 108867 A1 10 PLY.pts	0
Syncerus caffer ZMB Mam 108991 A329 13.pts	0
Syncerus caffer ZMB Mam 109009 A70 10.pts	0
Syncerus caffer ZMB Mam 19143.pts	0
Syncerus caffer ZMB Mam 29536.pts	0
Syncerus caffer ZMB Mam 35239.pts	0
Syncerus caffer ZMB Mam 41818.pts	0
Syncerus caffer ZMB Mam 41819.pts	0
Syncerus caffer ZMB Mam 41820.pts	0

APPENDIX 2. — UPGMA cluster dendrograms of the cranial landmark coordinates for **A** all specimens (Bovini), and **B** *Ugandax* Cooke & Coryndon, 1970 and *Syncerus* Hodgson, 1847. African fossil taxa highlighted in **bold**. OMO 53-10001 plots close to individuals of *Sy. caffer* (Sparrman, 1779) in **A**. The high similarity of *Pelorovis* Reck, 1928, *Simatherium* Dietrich, 1941, and one specimen of *Sy. antiquus* (Duvernoy, 1851) to each other in **A** suggests artifacts of cranial deformation might be affecting the cranial shape of these specimens.

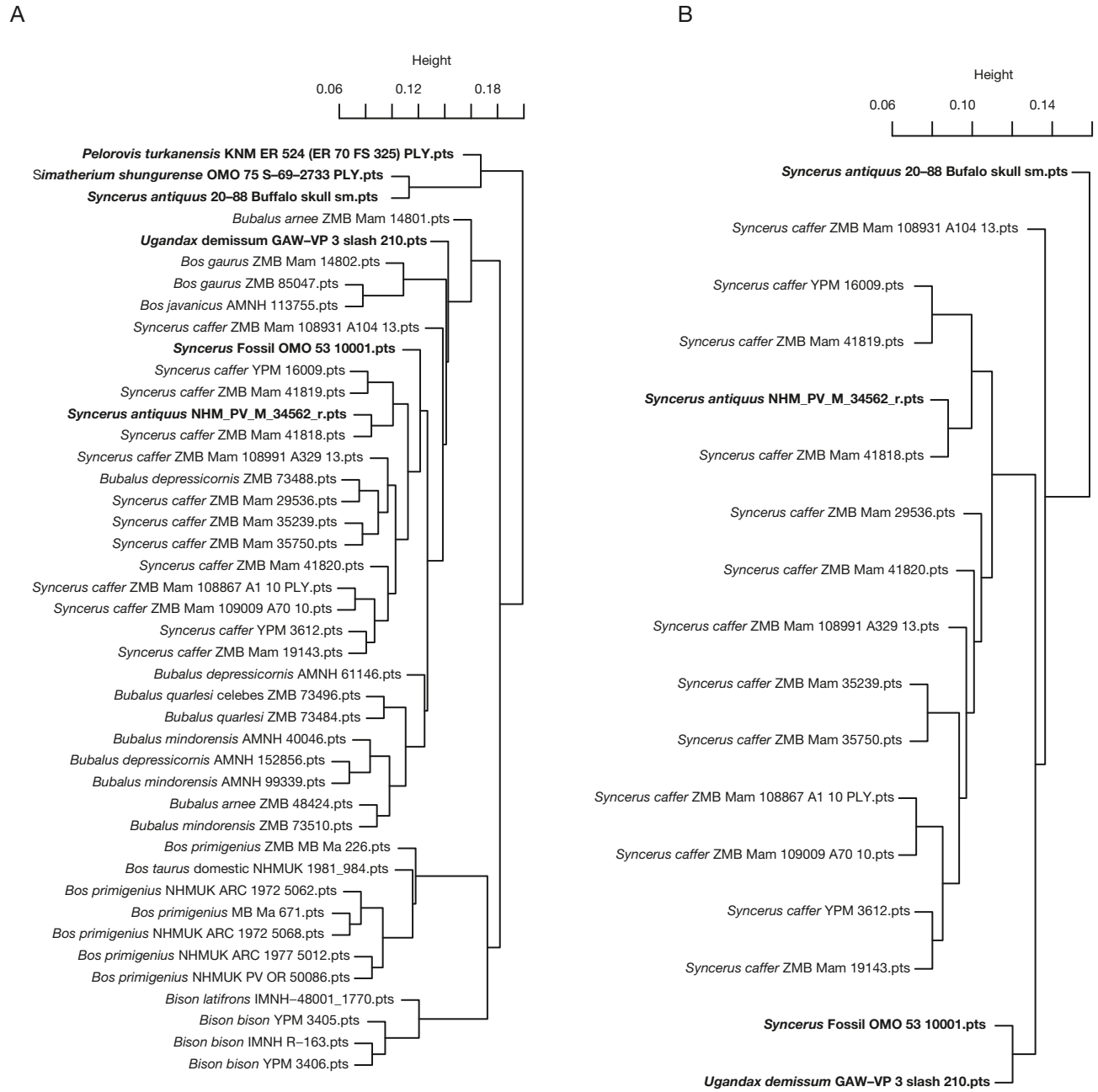

Appendix 3. — The first four principal components of cranial shape in Bovini. Same as Figure 8, but with taxon labels. Abbreviations: **Bo bis**, *Bos bison*; **Bo gau**, *Bos gaurus*; **Bo jav**, *Bos javanicus*; **Bo lati**, *Bos latifrons*; **Bo pri**, *Bos primigenius*; **Bo tau**, *Bos primigenius* (domestic); **Bu arn**, *Bubalus arnee*; **Bu dep**, *Bubalus depressicornis*; **Bu min**, *Bubalus mindorensis*; **Bu qua**, *Bubalus quarlesi*; **Pe tur**, *Pelorovis turkanensis*; **Si shu**, *Simatherium shungurense*; **Sy ant**, *Syncerus antiquus*; **Sy caf**, *Syncerus caffer*; **Sy n. sp.**, *Syncerus ekosowan* n. sp.; **Ug dem**, *Ugandax demissum*.

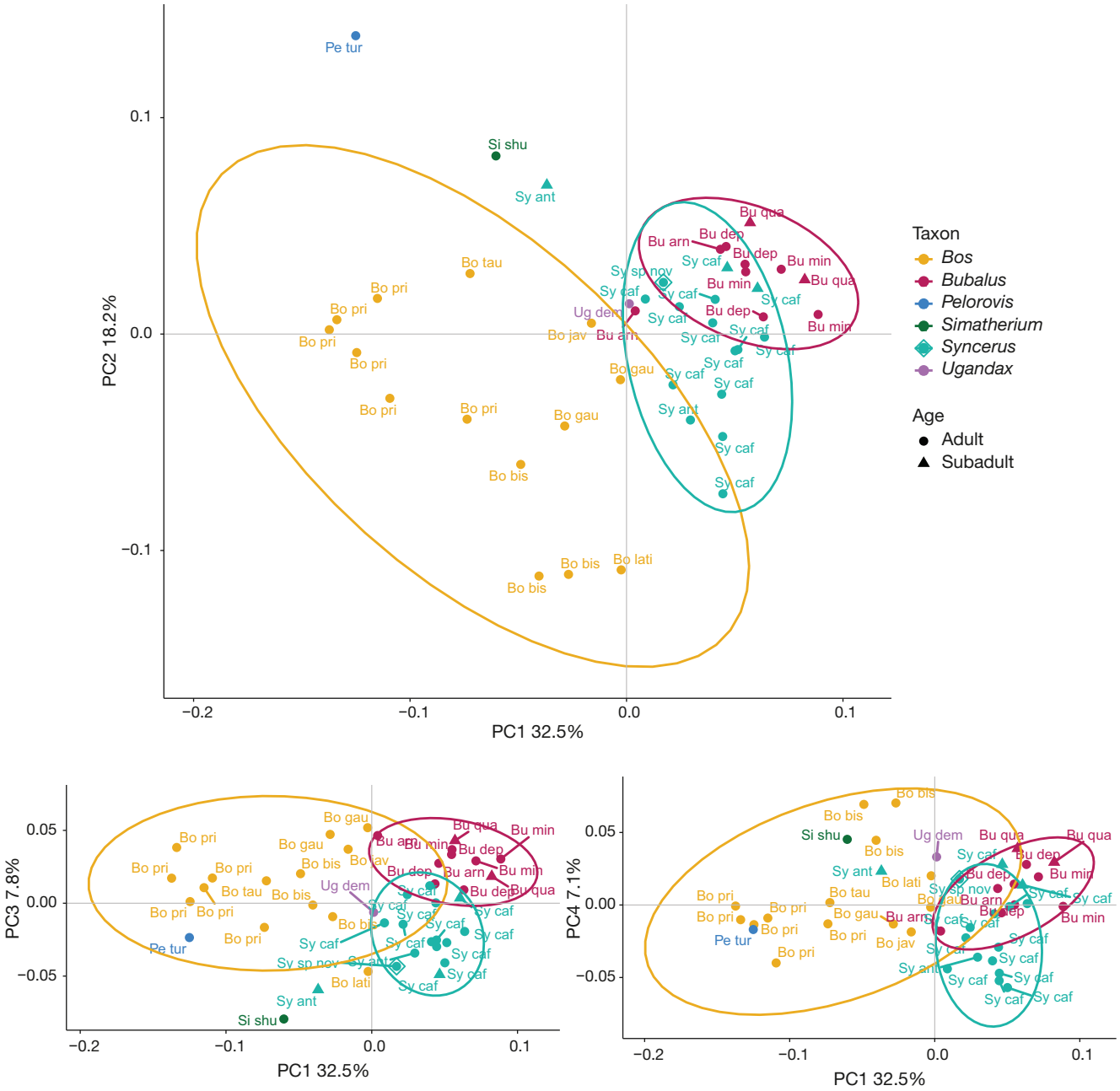

Appendix 4. — The first four principal components of cranial shape in Bovini. Same as Figure 8 but using the bilaterally symmetric shape component. Similar results indicate that the inclusion of fossil specimens (which might have some degree of bilaterally asymmetric deformation) is not significantly affecting the results.

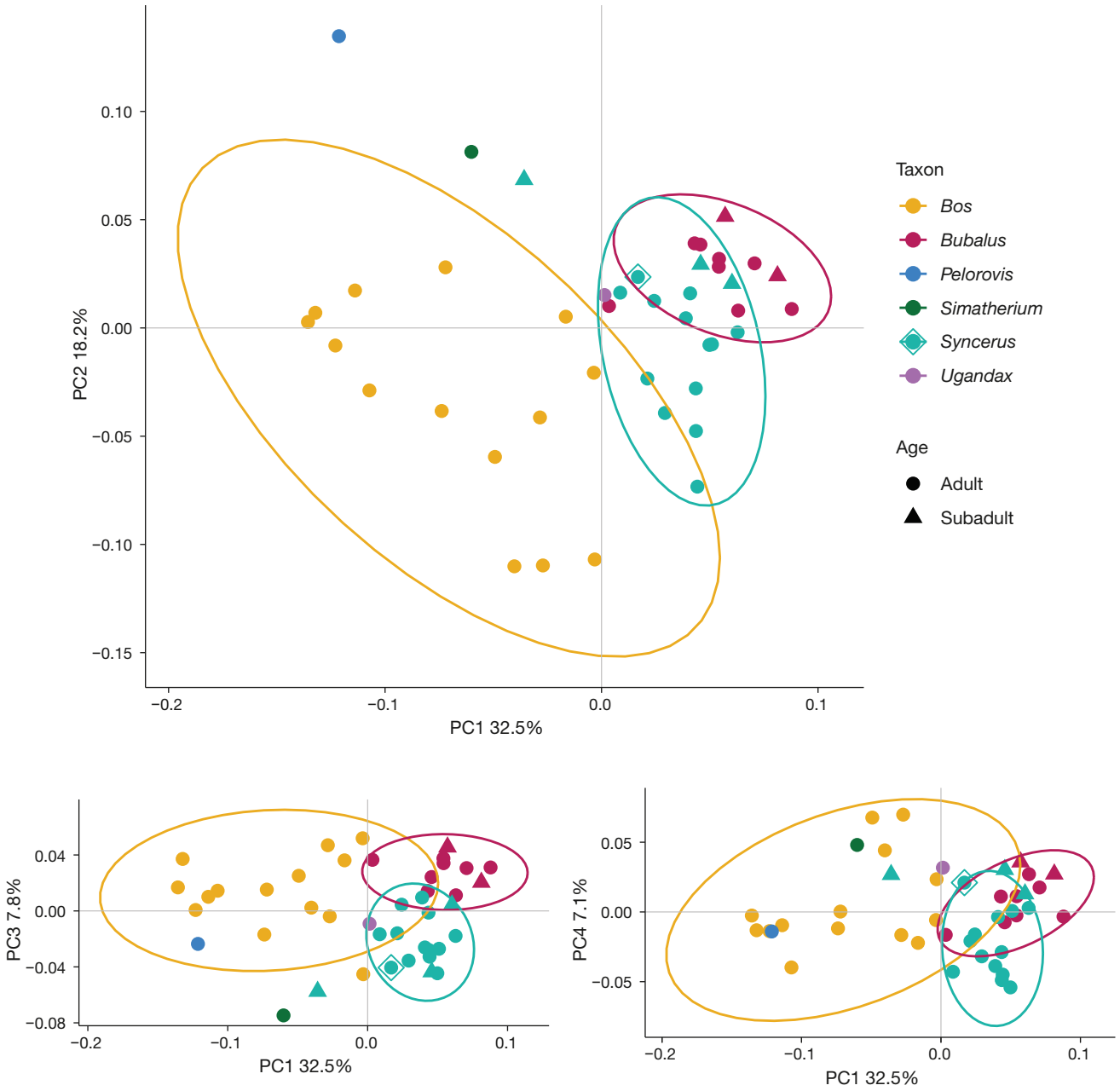

APPENDIX 5. — The first four principal components of cranial shape in Bovini. Same as Figure 8 but with fossil specimens removed prior to the analysis. Similar results indicate that the inclusion of fossil specimens (some with deformation) is not significantly affecting the results.

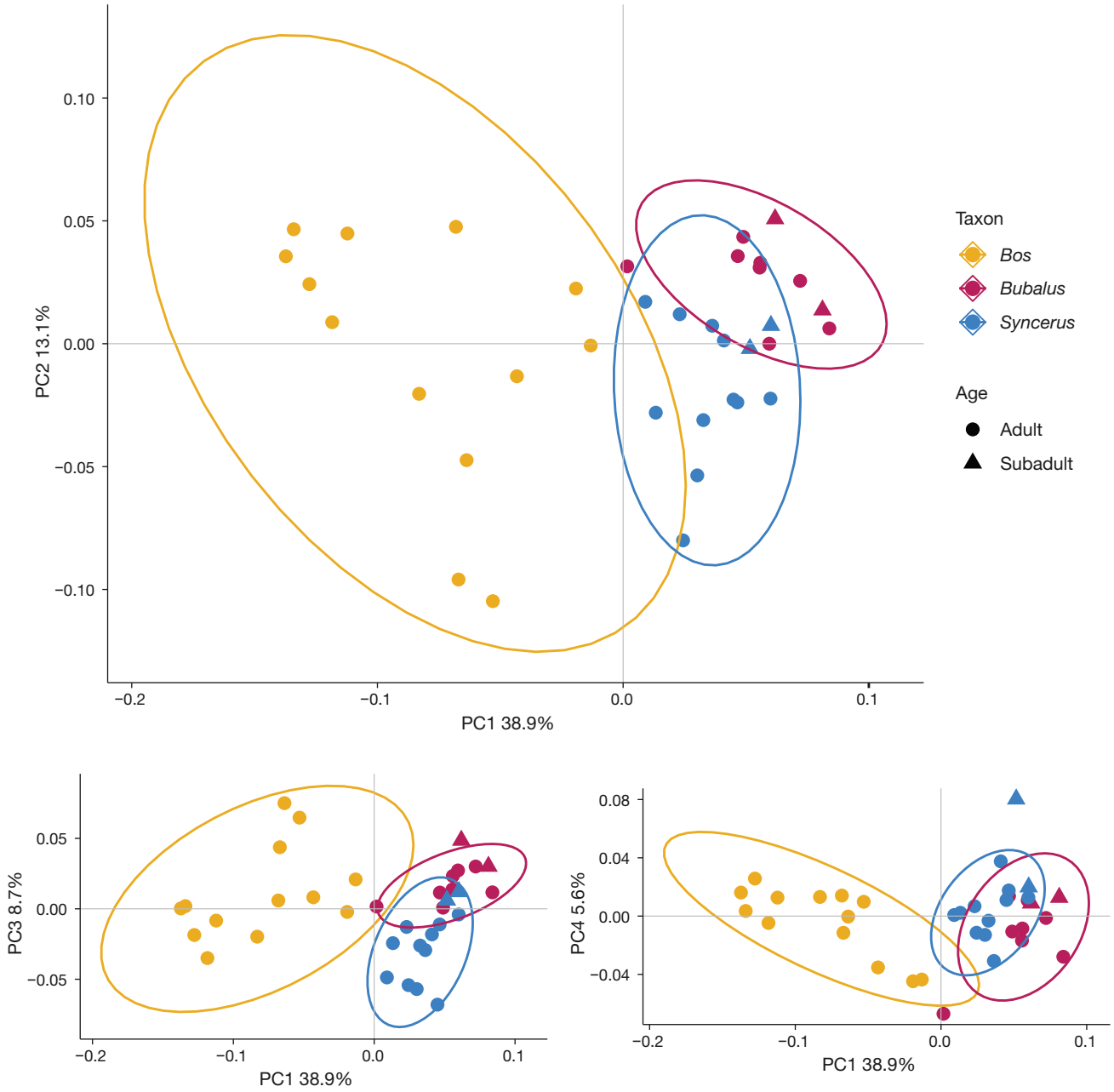

APPENDIX 6. — The first four principal components of cranial shape in Bovini. Same as Figure 8 but with landmarks for which data was missing for >5 specimens removed prior to the analysis (a reduction from 53 to 43 landmarks). Similar results indicate that the estimation of missing data is not significantly affecting the results.

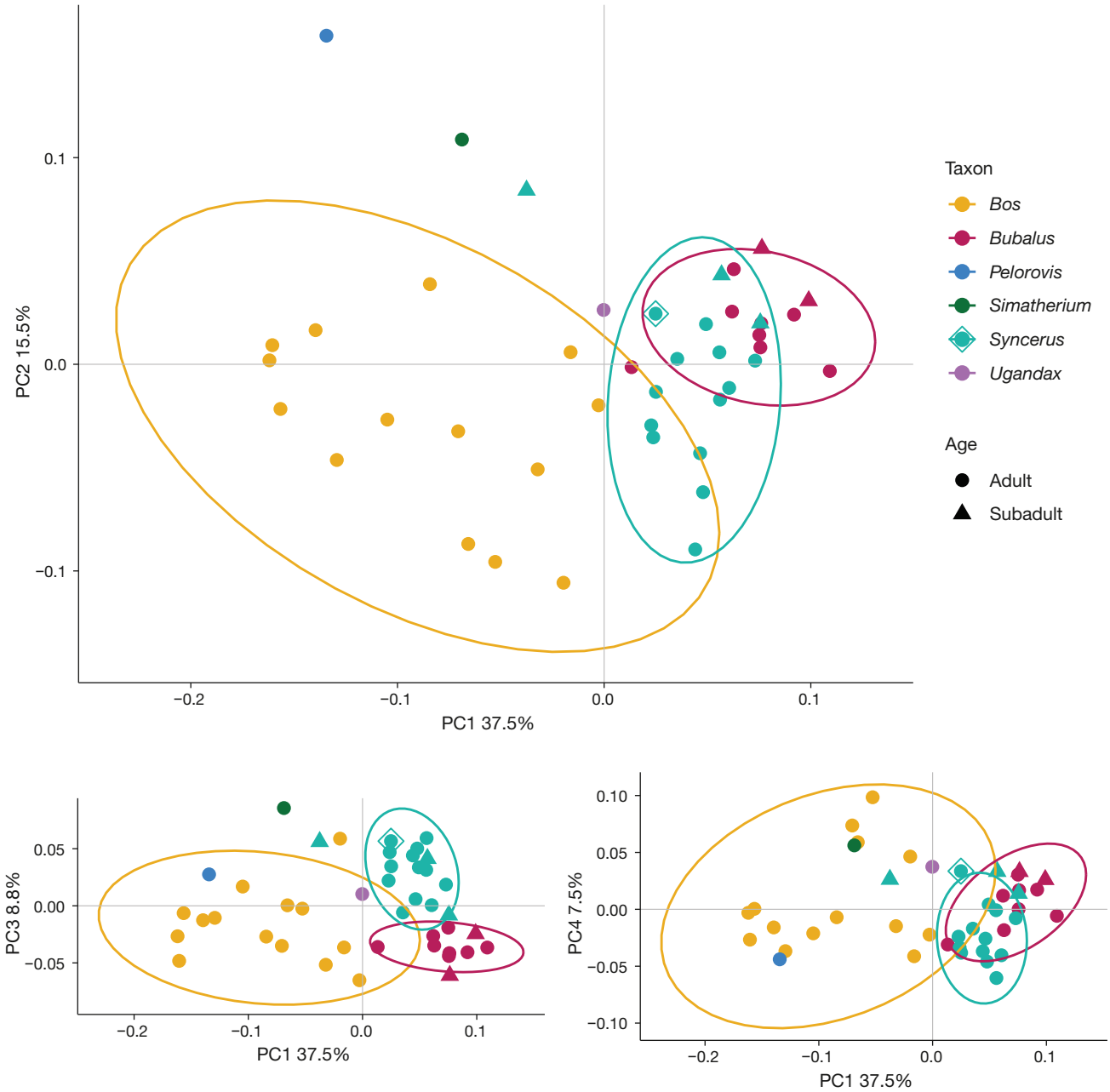

Appendix 7. — The first four principal components of cranial shape in Bovini. Same as Figure 8 but with all landmarks which were missing in Omo 53-10001 removed prior to the analysis (largely from the anterior snout region, a reduction from 53 to 43 landmarks). Similar results indicate that the estimation of missing landmarks is not significantly affecting the results.

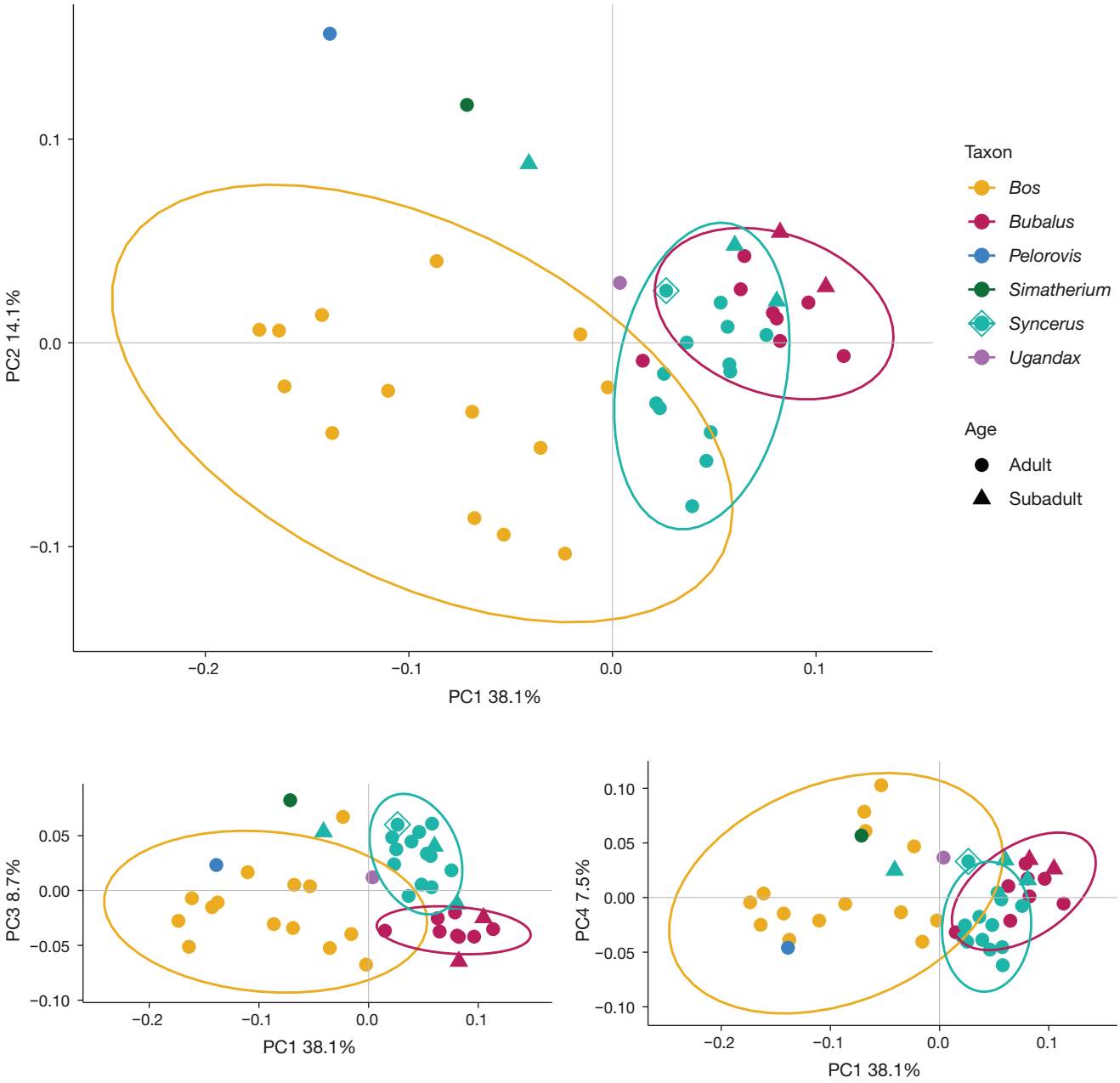

APPENDIX 8. — Shape changes associated with the first three principal components: **A**, all Bovini; **B**, *Syncerus* spp. Same as Figure 9 but with extant species and specimens only (fossil specimens removed prior to the analysis). Note the polarity of the first principal component (**PC1**) in the analysis with *Syncerus* Hodgson, 1847 only has inverted, but otherwise shape change in both this and the analysis of all Bovini are largely similar.

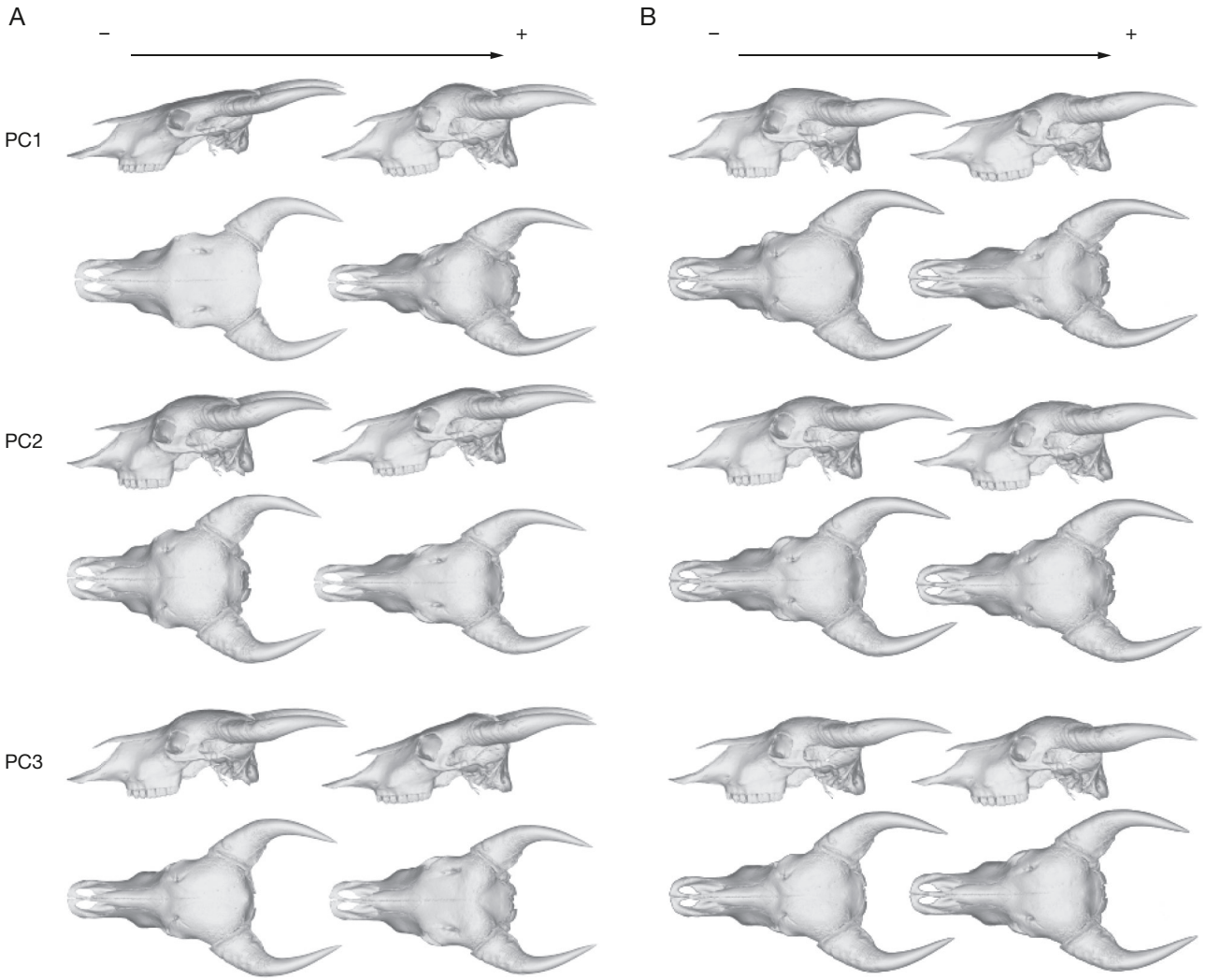

APPENDIX 9. — The first principal component (**PC1**) plotted against centroid size in: **A**, Bovini; **B**, *Syncerus* Hodgson, 1847 and *Ugandax* Cooke & Coryndon, 1970. Same as Figure 10, but with taxon and specimen labels. Abbreviations: **Bo bis**, *Bos bison*; **Bo gau**, *Bos gaurus*; **Bo jav**, *Bos javanicus*; **Bo lati**, *Bos latifrons*; **Bo pri**, *Bos primigenius*; **Bo tau**, *Bos primigenius* (domestic); **Bu arn**, *Bubalus arnee*; **Bu dep**, *Bubalus depressicornis*; **Bu min**, *Bubalus mindorensis*; **Bu qua**, *Bubalus quarlesi*; **Pe tur**, *Pelorovis turkanensis*; **Si shu**, *Simatherium shungurense*; **Sy ant**, *Syncerus antiquus*; **Sy caf**, *Syncerus caffer*; **Sy n. sp.**, *Syncerus ekosowan* n. sp.; **Ug dem**, *Ugandax demissum*.

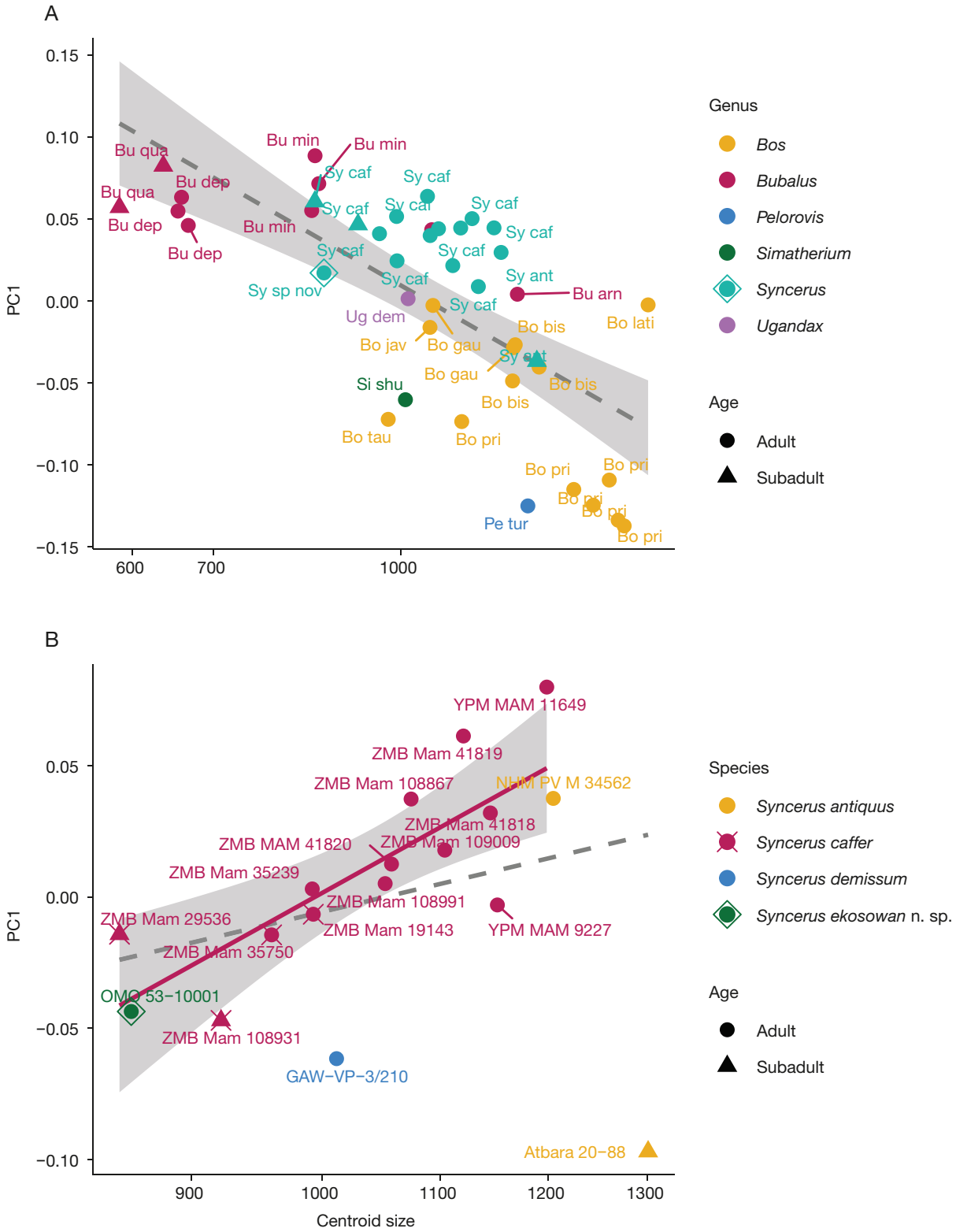

Appendix 10. — The first principal component (PC1) plotted against centroid size in: **A**, Bovini; **B**, *Syncerus* Hodgson, 1847 and *Ugandax* Cooke & Coryndon, 1970. Same as Figure 10, but with extant species and specimens only (fossil specimens removed prior to the analysis). Note the polarity of PC1 has inverted (also in Appendix 8), but the relationships among specimens remain largely the same. Abbreviations: **Bo bis**, *Bos bison*; **Bo gau**, *Bos gaurus*; **Bo jav**, *Bos javanicus*; **Bo lati**, *Bos latifrons*; **Bo pri**, *Bos primigenius*; **Bo tau**, *Bos primigenius* (domestic); **Bu arn**, *Bubalus arnee*; **Bu dep**, *Bubalus depressicornis*; **Bu min**, *Bubalus mindorensis*; **Bu qua**, *Bubalus quarlesi*; **Pe tur**, *Pelorovis turkanensis*; **Si shu**, *Simatherium shungurense*; **Sy ant**, *Syncerus antiquus*; **Sy caf**, *Syncerus caffer*; **Sy n. sp.**, *Syncerus ekosowan* n. sp.; **Ug dem**, *Ugandax demissum*.

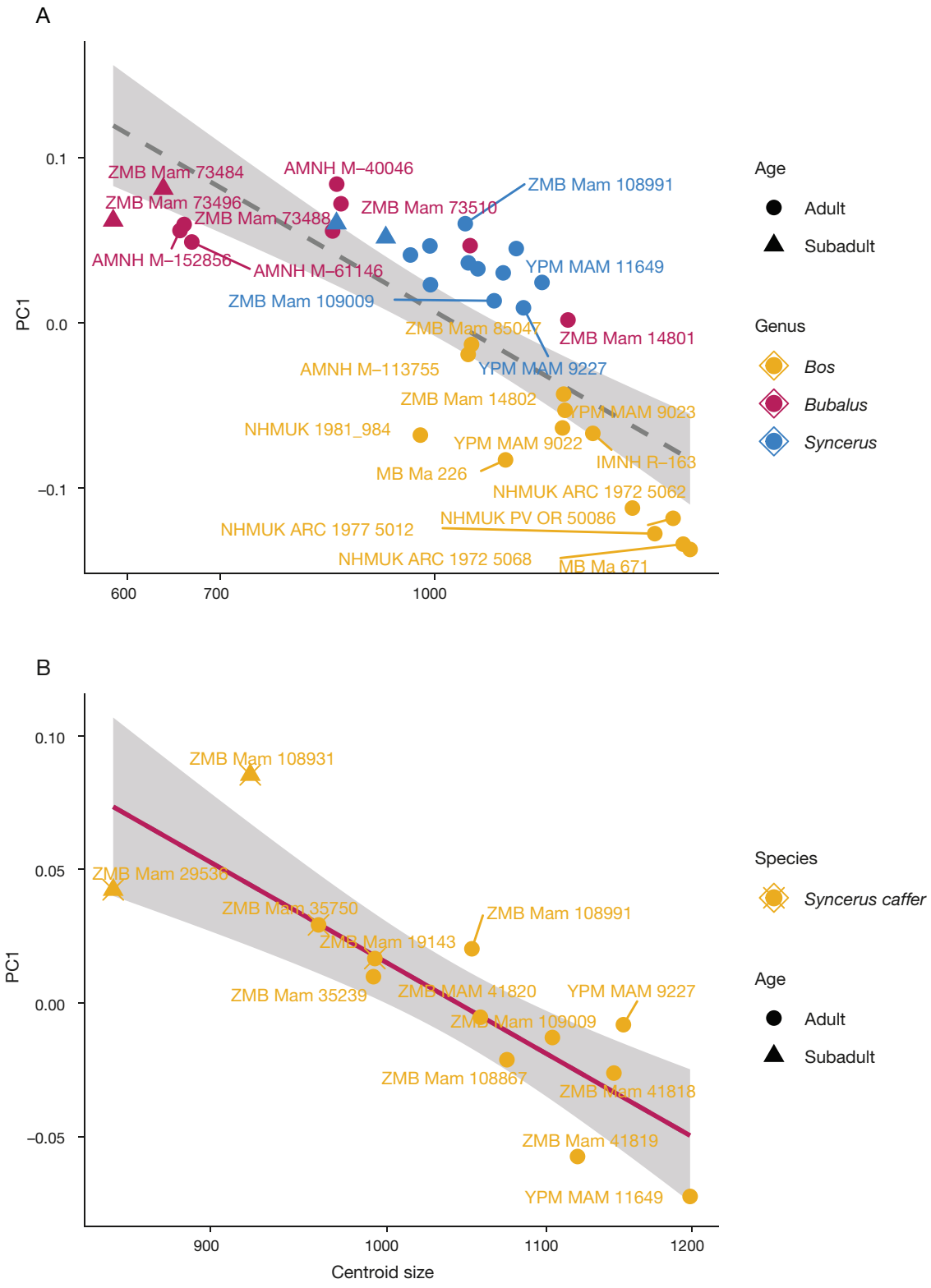

APPENDIX 11. — The regression score of cranial shape on log centroid size plotted against centroid size in: **A**, Bovini; **B**, *Ugandax* Cooke & Coryndon, 1970 and *Syncerus* Hodgson, 1847. Same as Figure 11, but with taxon and specimen labels. Abbreviations: **Bo bis**, *Bos bison*; **Bo gau**, *Bos gaurus*; **Bo jav**, *Bos javanicus*; **Bo lati**, *Bos latifrons*; **Bo pri**, *Bos primigenius*; **Bo tau**, *Bos primigenius* (domestic); **Bu arn**, *Bubalus arnee*; **Bu dep**, *Bubalus depressicornis*; **Bu min**, *Bubalus mindorensis*; **Bu qua**, *Bubalus quarlesi*; **Pe tur**, *Pelorovis turkanensis*; **Si shu**, *Simatherium shungurense*; **Sy ant**, *Syncerus antiquus*; **Sy caf**, *Syncerus caffer*; **Sy n. sp.**, *Syncerus ekosowan* n. sp.; **Ug dem**, *Ugandax demissum*.

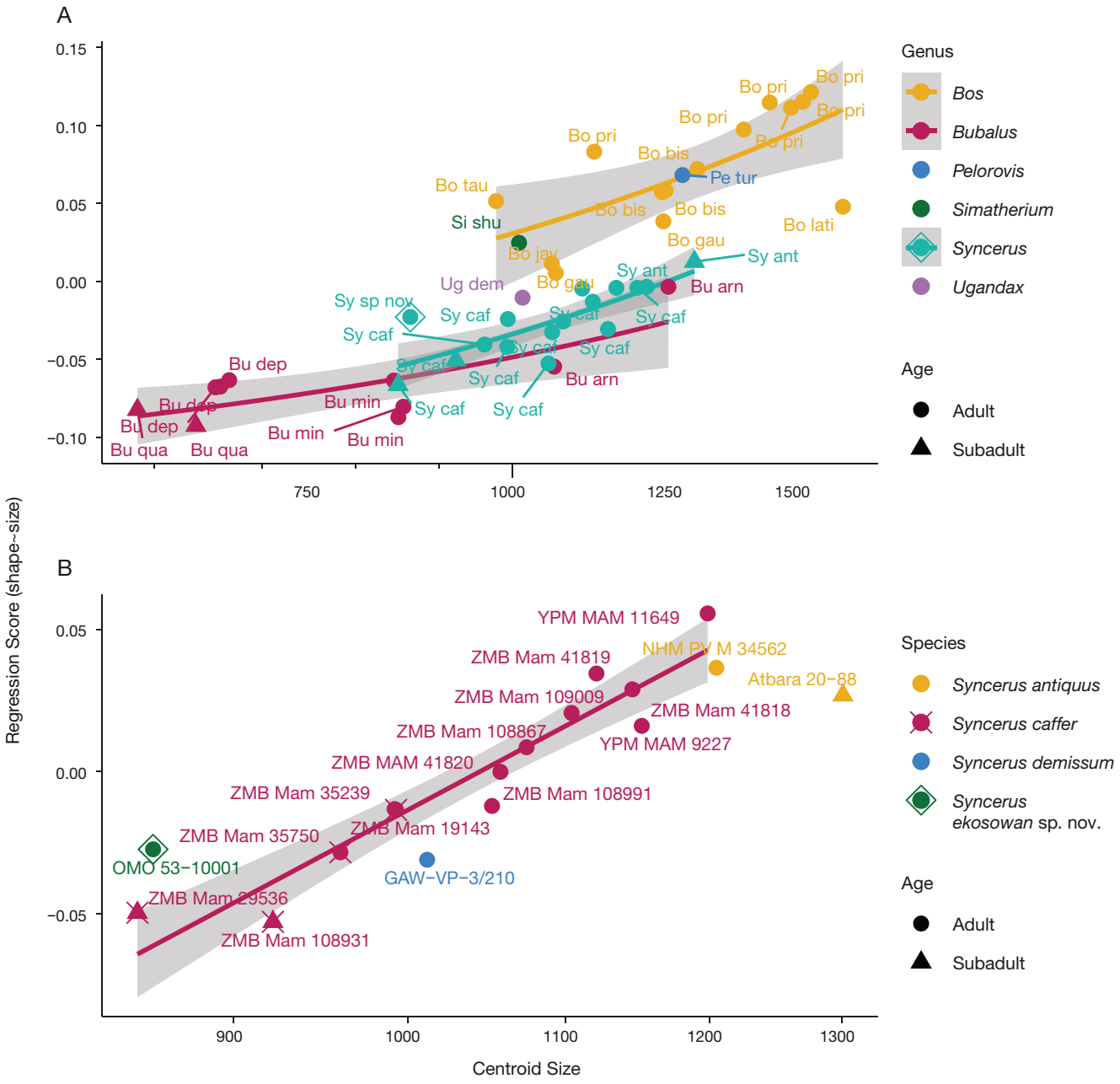

APPENDIX 12. — The regression score of cranial shape on log centroid size plotted against centroid size in: **A**, Bovini; **B**, *Syncerus* Hodgson, 1847. Same as Figure 11, but extant species only (fossil specimens removed prior to the analysis). Abbreviations: **Bo bis**, *Bos bison*; **Bo gau**, *Bos gaurus*; **Bo jav**, *Bos javanicus*; **Bo lati**, *Bos latifrons*; **Bo pri**, *Bos primigenius*; **Bo tau**, *Bos primigenius* (domestic); **Bu arn**, *Bubalus arnee*; **Bu dep**, *Bubalus depressicornis*; **Bu min**, *Bubalus mindorensis*; **Bu qua**, *Bubalus quarlesi*; **Pe tur**, *Pelorovis turkanensis*; **Si shu**, *Simatherium shungurense*; **Sy ant**, *Syncerus antiquus*; **Sy caf**, *Syncerus caffer*; **Sy n. sp.**, *Syncerus ekosowan* n. sp.; **Ug dem**, *Ugandax demissum*.

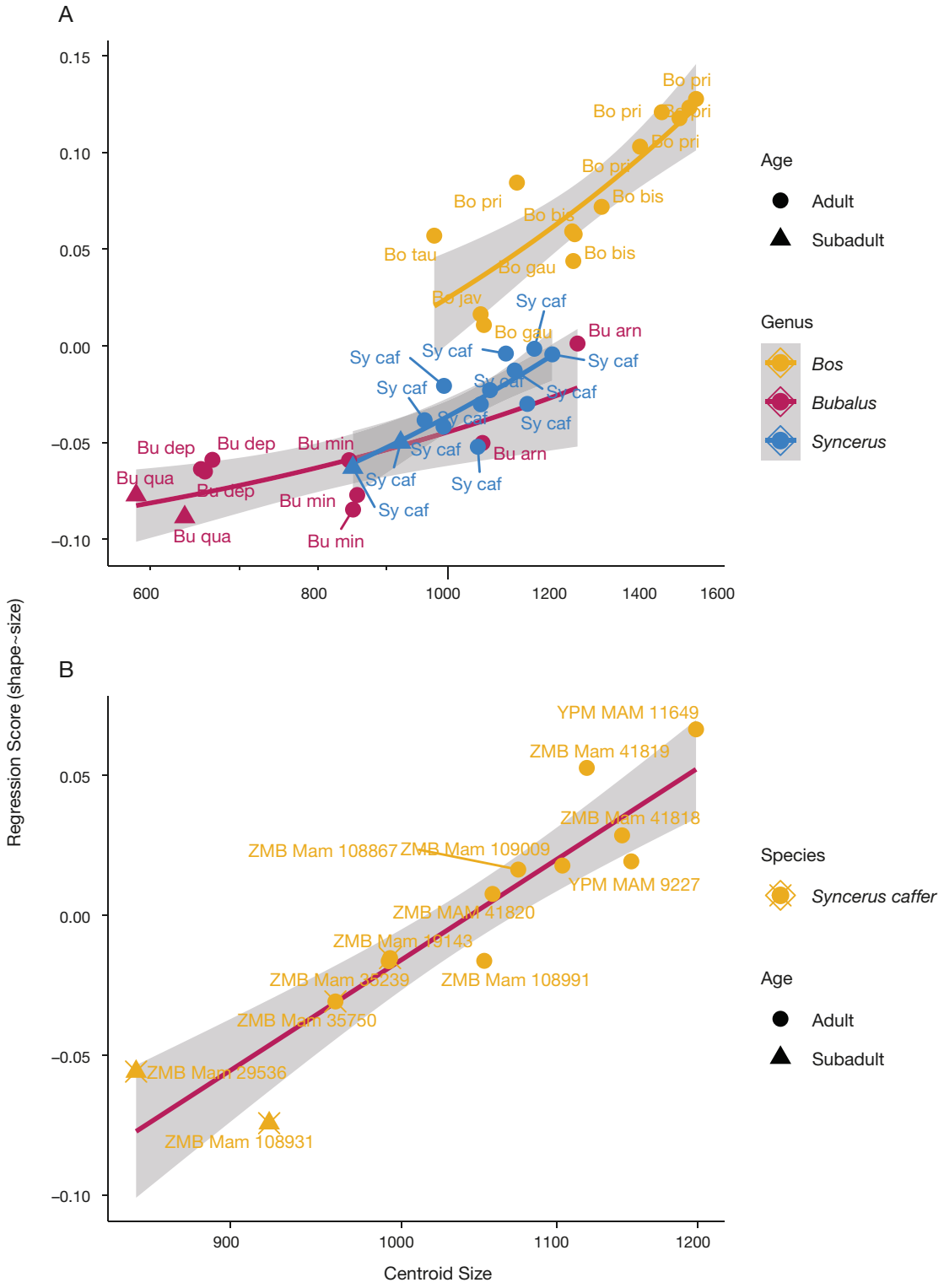

APPENDIX 13. — The first four principal components of cranial shape in *Ugandax* Cooke & Coryndon, 1970 and *Syncerus* spp. Same as Figure 12, with data points labelled by specimen number. Abbreviations: **Bo bis**, *Bos bison*; **Bo gau**, *Bos gaurus*; **Bo jav**, *Bos javanicus*; **Bo lati**, *Bos latifrons*; **Bo pri**, *Bos primigenius*; **Bo tau**, *Bos primigenius* (domestic); **Bu arn**, *Bubalus arnee*; **Bu dep**, *Bubalus depressicornis*; **Bu min**, *Bubalus mindorensis*; **Bu qua**, *Bubalus quarlesi*; **Pe tur**, *Pelorovis turkanensis*; **Si shu**, *Simatherium shungurense*; **Sy ant**, *Syncerus antiquus*; **Sy caf**, *Syncerus caffer*; **Sy n. sp.**, *Syncerus ekosowan* n. sp.; **Ug dem**, *Ugandax demissum*.

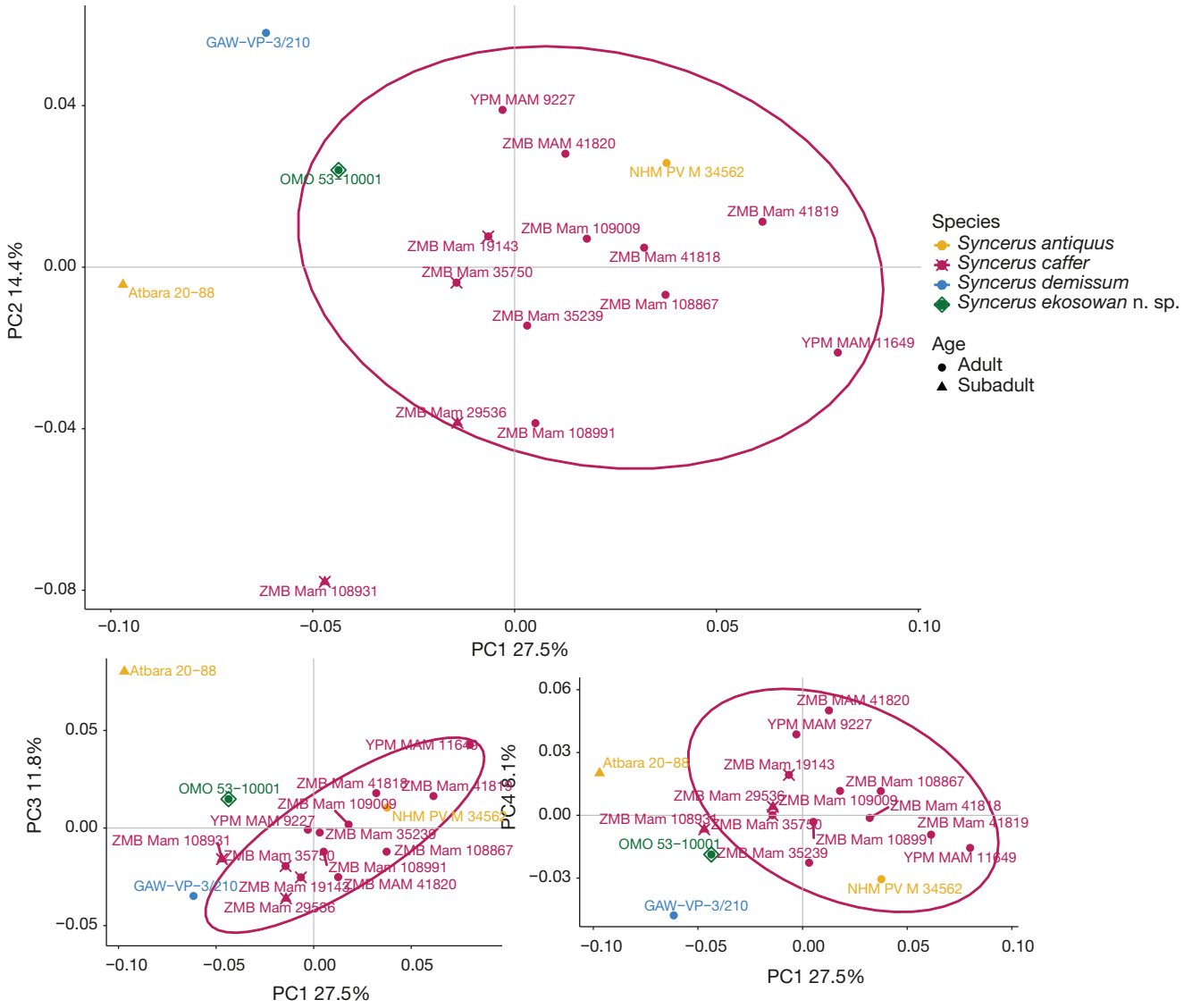

APPENDIX 14. — The first four principal components of cranial shape in *Syncerus* Hodgson, 1847. Same as Figure 12, but with *Syncerus caffer* (Sparrman, 1779) only (fossil specimens removed prior to the analysis).